
A CRITIQUE OF A VARIETY OF “MEMORY-BASED” PROCESS MONITORING METHODS

A PREPRINT

 **Sven Knoth**

Dep. of Mathematics & Statistics
Helmut Schmidt University
Hamburg, Germany
knoth@hsu-hh.de

 **Nesma A. Saleh**

Dep. of Statistics
Cairo University
Giza, Egypt
neasaleh@feps.edu.eg

 **Mahmoud A. Mahmoud**

Dep. of Statistics
Cairo University
Giza, Egypt
mamahmou@feps.edu.eg

 **William H. Woodall**

Dep. of Statistics
Virginia Tech
Blacksburg VA, USA
bwoodall@vt.edu

 **Victor G. Tercero-Gómez**

School of Engineering & Sciences
Tecnologico de Monterrey
Monterrey, Nuevo Leon, Mexico
victor.tercero@tec.mx

October 20, 2021

Abstract

Many extensions and modifications have been made to standard process monitoring methods such as the exponentially weighted moving average (EWMA) chart and the cumulative sum (CUSUM) chart. In addition, new schemes have been proposed based on alternative weighting of past data, usually to put greater emphasis on past data and less weight on current and recent data. In other cases, the output of one process monitoring method, such as the EWMA statistic, is used as the input to another method, such as the CUSUM chart. Often the recursive formula for a control chart statistic is itself used recursively to form a new control chart statistic. We find the use of these ad hoc methods to be unjustified. Statistical performance comparisons justifying the use of these methods have been either flawed by focusing only on zero-state run length metrics or by making comparisons to an unnecessarily weak competitor.

Keywords Control chart · Cumulative sum (CUSUM) chart · Exponentially weighted moving average (EWMA) chart · Mixed control charts · Statistical process monitoring

1 Introduction

Many extensions and modifications have been made recently to standard process monitoring methods such as the exponentially weighted moving average (EWMA) chart and the cumulative sum (CUSUM) chart. We find that many of these methods add complications with no benefits in terms of statistical performance. In addition, new schemes have been proposed based on alternative weighting of past data, usually to put greater emphasis on past data and less weight on current and recent data. Some of these methods, the homogeneously weighted moving average (HWMA) chart, the progressive mean (PM) chart, and the generally weighted moving average (GWMA) chart, have already been studied by [Knoth, Tercero-Gómez, Khakifirooz, and Woodall \[2021a\]](#) and [Knoth, Woodall, and Tercero-Gómez \[2021b\]](#), and found to be flawed and unnecessary.

We consider in our paper what we refer to as compound charts. These include what are referred to in the literature as mixed or hybrid charts. In these cases the output of one process monitoring method, such as the EWMA or moving average (MA) statistic, is used as the input to another method, such as the CUSUM chart. Increasingly the recursive formula for a control chart statistic is itself used recursively as with the double and

triple EWMA charts. We find these methods to be ad hoc, unnecessary, inadequately justified, and often with unreasonable weighting patterns for data where the past data values are given more weight than the present ones. Past comparisons justifying the use of these methods are either based on zero-state run length performance instead of the more realistic steady-state performance, on comparisons made to an unnecessarily weak competitor, or both.

What have been referred to in the literature as “mixed” control charts should not to be confused with the simultaneous use of more than one control chart such as the use of several cumulative sum (CUSUM) charts with different reference values or the use of a Shewhart chart in conjunction with a CUSUM chart, as proposed by Lucas [1982]. Instead, mixed charts involve the use of the control chart statistic of one chart as input into the control chart statistic or rule of another chart. Riaz et al. [2011a], Abbas et al. [2011], and Abbas et al. [2015] have proposed using runs rules with EWMA and CUSUM charts. These methods fit into our framework.

We aim in this article to provide an extensive review of the literature on the compound control charts. We also show that a proper performance comparison of these charts to the conventional ones shows the added complications provide no benefits. We evaluate the proposed charts in terms of the more realistic steady-state performance and the conditional expected delay (CED). We note that with compound charts, a Markov chain approach is no longer easily derived. We also show that the use of the standard design parameter values of the conventional methods (e.g. observations’ weights) provides misleading comparisons and conclusions since these compound approaches change the usual weighting structure on past and current observations.

Most of the papers we review on compound charts have been published in the last five years. We obviously cannot study the performance of all of these methods, so we chose to study in detail only five of them as illustrations. These are the mixed EWMA-CUSUM chart proposed by Abbas et al. [2013], the use of runs rules with CUSUM and EWMA charts, the double moving average (DMA) chart of Khoo and Wong [2008], the double EWMA (DEWMA) chart of Shamma et al. [1991] and Shamma and Shamma [1992], and the double PM (DPM) of Abbas et al. [2019].

The paper is organized as follows. In Section 2, we provide an extensive literature review on the proposed compound charts; namely the recursive EWMA charts, memory-type charts with run rules, MA, PM, HWMA, and mixed control charts. Afterwards, we provide some basic notation in Section 3. We re-evaluate each of the mixed EWMA-CUSUM, RR-CUSUM/EWMA, DMA, DEWMA, and DPM methods in Sections 4, 5, 6, 7, and 8, respectively, in terms of their zero- and steady-state performance and their CED behavior. In Section 9, we provide our concluding remarks.

2 Literature Review

2.1 Recursive use of the EWMA statistic

A recursive use of the EWMA statistic implies switching the EWMA chart statistic formula into a recursive function; by which it keeps calling itself as a function input in a repeated manner. Shamma and Shamma [1992] introduced a double EWMA (DEWMA) chart, while Alevizakos et al. [2021a] introduced a triple EWMA (TEWMA) chart. Haq [2013] introduced a hybrid EWMA (HEWMA) chart which is equivalent in structure and concept to the DEWMA chart. Haq [2017] noted that the variance of the chart statistic derived in Haq [2013] was incorrect, and provided the correct formula. Throughout this section, the DEWMA chart terminology will also be used to refer to the HEWMA chart since the DEWMA and HEWMA charts are equivalent.

By expanding the statistics of these proposed charts into weighted averages, one can easily realize that they are fundamentally flawed in that they give past data values more weight than current values. As discussed by Lai [1974], for example, the weight given to a particular data value should not increase as the data value ages. This undesirable characteristic does not adversely affect zero-state run length performance, but it can result in poor steady-state run length performance. Many other compound charts based on recursive use of control chart statistic formulas share this property. Virtually all performance comparisons justifying compound charts are based on the less realistic zero-state performance metrics under the assumption that any process shift occurs immediately as monitoring begins. Giving more weight to past data values than to current data values is clearly not reasonable in process monitoring applications.

Performance comparisons of the DEWMA or TEWMA chart with the EWMA chart typically use the same smoothing parameter for both methods. A more competitive EWMA chart would be one with a weighting scheme on past data similar to that of the DEWMA or TEWMA chart. Such comparisons then show

no performance benefits for the DEWMA or TEWMA chart. [Mahmoud and Woodall \[2010\]](#) extensively re-evaluated the DEWMA chart in comparison with the EWMA chart in terms of the zero-state performance with adjusted weights and worst-case (inertia-effect) performance. They concluded that the DEWMA chart shows a significantly weak performance in comparison to the EWMA chart because of the higher weights it gives to the older observations.

Despite its flaws, the DEWMA approach has been implemented in a number of applications. [Zhang and Chen \[2005\]](#) investigated the DEWMA chart in comparison with the EWMA chart to identify the range of shifts where the former surpasses the latter. They additionally provided some design values for the DEWMA chart. [Alkahtani \[2013\]](#) investigated the robustness of the DEWMA chart under non-normality, and [Nawaz et al. \[2021\]](#) studied the effect of non-normality on its performance. [Raji et al. \[2018\]](#) evaluated the use of some robust estimators in monitoring the process location parameters instead of the simple sample mean under known and estimated process parameters. [Ahmed et al. \[2020\]](#) integrated the DEWMA chart with a generalized least-squares (GLS) algorithm based on order statistics to develop a robust DEWMA chart to monitor non-normal processes.

[Perez Abreu and Schaffer \[2017\]](#) used a DEWMA chart to monitor linear drifts/shifts in the quality characteristic of interest. [Asif et al. \[2020\]](#) incorporated measurement error into the model used with the chart, while [Noor et al. \[2020\]](#) took a Bayesian approach with it. [Noor-ul Amin et al. \[2019\]](#), [Raza et al. \[2019\]](#), [Tariq et al. \[2020\]](#), and [Haq et al. \[2021\]](#) incorporated auxiliary information into the DEWMA chart; with [Raza et al. \[2019\]](#) considering two auxiliary variables. Auxiliary variables are those that are highly correlated with the variable of interest. It is assumed that the parameters of the distribution of the auxiliary variables are both known and cannot change over time. In survey sampling literature, such variables are used to increase the efficiency of the estimators of the population parameters. The required assumptions are unlikely to hold in process monitoring applications, as discussed by [Saleh et al. \[2021\]](#).

[Khoo et al. \[2010\]](#) proposed a Max-DEWMA chart which is based on the maximum of two DEWMA statistics to detect simultaneously changes in the process mean and variance. [Javaid et al. \[2020\]](#) evaluated it in the presence of auxiliary information, while [Javaid et al. \[2021\]](#) evaluated it in the presence of both measurement errors and auxiliary information. Further, for simultaneous monitoring of the process mean and dispersion, [Teh et al. \[2011\]](#) proposed a sum of squares DEWMA (SS-DEWMA) chart. In the SS-charts, two chart statistics are used; one for the process mean and one for the process variance, and the final chart statistic by which the status of the process is determined is based on the sum of squares of both statistics. [Ali and Haq \[2017\]](#) and [Tariq et al. \[2019\]](#) developed a DEWMA chart for monitoring only the process variance, while [Aslam et al. \[2019a\]](#) developed a proportion-DEWMA chart to monitor the process variance under non-normal or unknown (nonparametric) distributed processes.

[Azam et al. \[2015\]](#) and [Adeoti \[2018\]](#) added a repetitive sampling feature to the DEWMA chart. A repetitive sampling feature allows for taking additional samples at a given time point when the results of the drawn sample are indecisive. [Shafiq and Musliyar \[2018\]](#) corrected and recalculated some designs provided incorrectly in [Azam et al.'s \(2015\)](#) article. [Noor-ul Amin et al. \[2020\]](#) evaluated the DEWMA chart under different ranked set sampling (RSS) schemes; which are classical RSS, Extreme RSS (ERSS), Median RSS (MRSS), and Quartile RSS (QRSS). The RSS is a sampling scheme that depends on ranking the collected items when the actual measurements are difficult to make [[McIntyre, 1952](#)]. [Riaz and Abbasi \[2016\]](#) and [Raza et al. \[2020a\]](#) developed a nonparametric DEWMA chart for monitoring the process location parameter, and [Shafqat et al. \[2020\]](#) integrated the repetitive sampling technique with it. [Chan et al. \[2021\]](#) developed a distribution-free DEWMA chart based on the Lepage statistic to monitor simultaneously the process location and scale parameters.

On the attribute variable side, [Zhang et al. \[2003a\]](#) evaluated the DEWMA chart under Poisson processes. [Aslam et al. \[2016a\]](#) applied the chart on monitoring processes that use attribute and variable inspection at the same time. [Aslam et al. \[2018a\]](#) and [Alevizakos and Koukouvinos \[2019\]](#) developed a DEWMA chart to monitor the parameters of the Conway-Maxwell-Poisson (COM) distribution. This distribution is used to represent under-dispersed and over-dispersed count data. [Alevizakos and Koukouvinos \[2020a\]](#) and [Alevizakos and Koukouvinos \[2021a\]](#) used a DEWMA chart to monitor zero-inflated Poisson (ZIP) and zero-inflated binomial (ZIB) distributed processes, respectively.

Other underlying process distributions were also considered. For example, [Alevizakos and Koukouvinos \[2020b\]](#), [Raza et al. \[2020b\]](#), and [Adeoti \[2020\]](#) used a DEWMA chart to monitor time between events (TBE) (gamma-distributed processes), Weibull data, and exponentially distributed processes, respectively. [Bizuneh and Wang \[2019\]](#) proposed a likelihood ratio based DEWMA chart to monitor the shape parameter of the inflated Pareto process.

Further extensions and applications were conducted by [Abdella et al. \[2016\]](#) who used the DEWMA chart for profile monitoring, and [Alkahtani and Schaffer \[2012\]](#) and [Kuvattana \[2020\]](#) who extended the doubling concept to the multivariate EWMA chart.

As for the TEWMA chart, [Alevizakos et al. \[2021b,c\]](#) developed a nonparametric version of the chart, while [Letshedi et al. \[2021\]](#) did the same but with adding an improved modified FIR (IMFIR) feature to the chart to monitor changes in process location. [Alevizakos et al. \[2021d\]](#) proposed the use of a TEWMA chart to monitor the TBE (gamma-distributed processes). [Chatterjee et al. \[2021\]](#) used a TEWMA chart for monitoring process dispersion.

[Ali et al. \[2021a\]](#) developed a conditional expected value (CEV) hybrid DEWMA (CEVHDEWMA) chart for monitoring the mean of a Weibull distributed process under type-I censoring. The structure/concept of the HDEWMA chart is equivalent to the TEWMA chart.

We note here that the generally weighted moving average (GWMA) chart of [Sheu and Lin \[2003\]](#) is a generalization of the EWMA chart. Generally, [Mabude et al. \[2021\]](#) provided an extensive review on GWMA control charts. These charts were studied by [Knoth et al. \[2021b\]](#) and shown to have no advantages over the much simpler EWMA chart.

Nevertheless, a recursive use of the GWMA statistic was also proposed and used in different applications in the literature. For example, [Sheu and Hsieh \[2009\]](#) proposed a double version of the GWMA chart; namely the DGWMA chart, for detecting mean shifts. [Chiu and Sheu \[2008\]](#) and [Chiu and Lu \[2015\]](#) evaluated the DGWMA chart under Poisson-distributed processes, while [Chen \[2020\]](#) developed a DGWMA for monitoring COM-Poisson distributed processes. [Huang et al. \[2014\]](#) developed a sum of squares DGWMA (SS-DGWMA) chart. [Alevizakos et al. \[2019\]](#) proposed a one-sided DGWMA chart for monitoring TBE data (gamma-distributed). [Lu \[2018\]](#) proposed a sign-based non-parametric DGWMA chart when the process distribution is unknown, while [Karakani et al. \[2019\]](#) developed an exceedance test based DGWMA chart.

To illustrate the flaws of these methods, we consider the performance of the the DEWMA and TEWMA charts in Section 7.

2.2 Memory-type Control Charts with Run Rules

[Abbas et al. \[2011\]](#) were the first to introduce the use of run rules with a memory-type control chart. They proposed two run rules schemes to be applied on the EWMA chart. [Abbas et al. \[2015\]](#) noted some mistakenly calculated performance measures in [Abbas et al. \[2011\]](#) and provided the correct figures. By this correction, they noted a decrease in the strength of this proposed chart from that reported in [Abbas et al. \[2011\]](#). [Khoo et al. \[2016\]](#) extended the study of [Abbas et al. \[2011\]](#) by applying a Markov chain procedure to compute the performance measures. They suggested further run rules schemes than those proposed in [Abbas et al. \[2011\]](#). [Maravelakis et al. \[2019\]](#) derived double integral equations for computing the performance measures of an EWMA chart with run rules. [Arshad et al. \[2017\]](#) proposed the simultaneous use of runs rules (nine different schemes) and auxiliary information when monitoring the location parameter using an EWMA chart.

[Riaz et al. \[2011b\]](#) proposed two run rules schemes for the CUSUM charts. [Abbasi et al. \[2012\]](#) added some run rules to a scale CUSUM chart designed to monitor the process variability. [Adeoti and Malela-Majika \[2020\]](#) considered adding some supplementary run rules to the DEWMA chart design structure for monitoring the process mean. We consider the use of run rules with the CUSUM and EWMA charts in Section 5. Again we show that these complications add no performance benefits.

2.3 Moving Average Methods

A moving average (MA) control chart is based on the average of the last specified number of observations [[Roberts, 1966](#)]. The MA chart is known to be less sensitive than the EWMA and CUSUM charts for small shift sizes [[Wong et al., 2004](#), [Alevizakos et al., 2020](#)]. [Zhang et al. \[2004\]](#) noted that the derivation of the ARL formula of the MA chart provided in the literature – especially by [Wetherill and Brown \[1991\]](#) – is incomplete, and hence the formula is incorrect. [Zhang et al. \[2004\]](#) showed that this incorrect formula could just lead to an upper bound for the ARL value. They derived another formula, but it was not exact. It just provides a sharper upper bound for the ARL value. In their opinion, there is no exact formula that can be found for the ARL metric of the MA charts.

Similar to the DEWMA chart construction, [Khoo and Wong \[2008\]](#) introduced a double MA (DMA) chart. [Alevizakos et al. \[2020\]](#) noted that the derivation of the DMA chart statistic variance proposed by [Khoo and Wong \[2008\]](#) is incorrect and provided the correct formula. They re-evaluated the chart as well with the

corrected variance. They concluded that the DMA chart is more efficient than the EWMA and CUSUM charts only for the large shift sizes.

Several evaluations were conducted on the DMA chart. For example, [Areepong and Sukparungsee \[2011\]](#) and [Sukparungsee and Areepong \[2014\]](#) evaluated it under binomial processes, [Sukparungsee \[2013\]](#) under ZIP processes, and [Areepong and Sukparungsee \[2015\]](#) and [Areepong \[2016\]](#) under ZIB processes. [Phantu et al. \[2016\]](#) designed it for monitoring a ZIB model when the underlying distribution is the ratio of two Poisson means. [Phantu et al. \[2018\]](#) extended the latter study to develop a DMA chart to monitor Poisson processes modeled by an INAR(1) model, while [Raweesawat and Sukparungsee \[2021\]](#) provided some explicit formulas for calculating its ARL when designed to monitor a ZIP-INAR(1) model. [Areepong and Chananet \[2021\]](#) considered a DMA chart while monitoring zero-truncated Poisson processes.

[Adeoti et al. \[2019\]](#) proposed the use of a DMA chart to monitor process variability using the sample standard deviation. [Amir et al. \[2021\]](#) studied the use of the chart when there is auxiliary information. Recently, [Alevizakos et al. \[2021e,f\]](#) proposed triple MA (TMA) and quadruple MA (QMA) charts, respectively. Yet, these compound charts give increasingly more weight to past data values relative to the current data values than the DMA chart, making their use even more inadvisable. We consider the DMA chart performance in Section 6.

2.4 The Progressive Mean Approach

Progressive mean (PM) charts, originally proposed by [Abbas et al. \[2012\]](#), are based on the average of all data values obtained during process monitoring. Thus, each data value is given equal weight. [Abbas \[2015\]](#) suggested that a PM chart statistic can be looked at as a special case of the EWMA statistic with an adaptable smoothing parameter (reciprocal of the sample number); and hence can be treated as the Adaptive EWMA statistic proposed by [Capizzi and Masarotto \[2003\]](#). [Zafar et al. \[2021\]](#) negated the argument of [Abbas \[2015\]](#), and stated that the PM chart can neither be considered a special case of the EWMA chart nor of the AEWMA chart. This is because of the difference between the variances of the chart statistics, and that the weights are being updated only due to the change of the sample number, not the process status.

This approach showed considerable power to detect changes that occurred when the monitoring starts, but, as reviewed in [Knoth et al. \[2021a\]](#), it grossly under-performed when dealing with later changes. It should be noted that the “belief” approach of [Nezhad and Niaki \[2010\]](#) is also based on the average of all the process data collected. It thus shares the disadvantages of the PM chart. This approach has been used in various scenarios by [Aslam et al. \[2019b\]](#), [Shawky et al. \[2020\]](#) and [Aslam et al. \[2016b, 2017a\]](#).

On a recursive basis, [Abbas et al. \[2019\]](#) proposed a double PM (DPM) chart; which weights past data values more than current values. [Riaz et al. \[2021a\]](#) noted that the variance of the DPM chart statistic derived by [Abbas et al. \[2019\]](#) was incorrect due to some missing terms. [Riaz et al. \[2021a\]](#) derived the correct variance and re-evaluated the chart performance. They concluded that the chart based on the correct variance has much better performance than the older one.

[Alevizakos and Koukouvinos \[2020c\]](#) proposed a DPM chart to monitor mean shifts in Poisson processes. [Abbas et al. \[2021a\]](#) noted that the variance of the chart statistic derived by [Alevizakos and Koukouvinos \[2020c\]](#) is incorrect and provided a corrected one. [Abbas et al. \[2021b\]](#) introduced a sign-test based on nonparametric DPM control charts. [Alevizakos and Koukouvinos \[2021b\]](#) proposed the use of DPM chart to monitor TBE data which are modeled by a gamma distribution.

[Ajadi et al. \[2021\]](#) developed two multivariate progressive variance (PV) control charts; one uses the trace and another uses the eigenvalues of the variance-covariance matrix. The charts are evaluated under the assumption of known and unknown in-control process parameters.

Performance of the DPM approach is considered in Section 8.

2.5 Homogeneously Weighted Moving Average Methods

With the homogeneously weighted moving average (HWMA) approach of [Abbas \[2018\]](#), all past data values are weighted equally with the most current data value weighted differently. [Knoth et al. \[2021a\]](#) reviewed this approach and showed that its performance shares the disadvantages of the PM approach.

Double recursive versions (DHWMA charts) were proposed independently by [Abid et al. \[2020\]](#) and [Adeoti and Koleoso \[2020\]](#). [Alevizakos et al. \[2021g\]](#) developed another DHWMA chart to improve upon that proposed by [Abid et al. \[2020\]](#) and [Adeoti and Koleoso \[2020\]](#). Their justification was that the chart developed by [Abid](#)

et al. [2020] did not exactly imitate the procedure of Shamma and Shamma [1992] in developing the DEWMA chart. Because the chart developed by Adeoti and Koleoso [2020] has an incorrect variance, Malela-Majika et al. [2021] provided a corrected formula of the variance of the control chart statistic. Anwar et al. [2021a] applied the DHWMA chart when there is auxiliary information available. Riaz et al. [2021b] developed a nonparametric DHWMA chart using the sign test. Alevizakos et al. [2021h] developed a nonparametric DHWMA chart proposed by Alevizakos et al. [2021g] based on the sign test.

Generally, we note that the DHWMA [Abid et al., 2020, Riaz et al., 2021b] chart and the triple HWMA chart of Riaz et al. [2021c] are simply reparameterizations of the basic HWMA chart of Abid et al. [2020] and thus superfluous.

2.6 Mixed Control Charts

In mixed control charts, the chart statistic of one chart is used as input to another control chart. Many of these types of methods have been introduced since there are many types of charts and many ways of mixing them.

Abbas et al. [2013] was the first to propose mixing the EWMA and CUSUM charts; where they proposed using the EWMA statistic as an input in the CUSUM chart statistics. Following, Zaman et al. [2015] proposed the inverse version of Abbas et al. [2013] chart by which the CUSUM statistics are used as inputs in the EWMA chart statistic. Generally mixing these two charts has been used extensively. For example, Zaman et al. [2016] used this mix in monitoring process dispersion, and Zaman et al. [2017] used it in monitoring the process location and dispersion simultaneously. Ajadi et al. [2016] incorporated headstarts and runs rules into it. A comparison study of these mixed methods was reported by Nazir et al. [2016]. Abid et al. [2018] investigated the in-control robustness of this mix of the EWMA and CUSUM under non-normal and contaminated processes. Hussain et al. [2020] proposed a median version for process location monitoring. Anwar et al. [2020, 2021b] mixed the two charts with the incorporation of auxiliary information while Mohamadkhani and Amiri [2020] considered other sampling scenarios. Aslam [2016] mixed these charts for monitoring Weibull-distributed data. Malela-Majika and Rapoo [2017] developed a distribution free version, and Osei-Aning et al. [2017] extended the approach to autocorrelated data. Abbas et al. [2018] proposed mixing an EWMA statistic with a dual CUSUM chart, Riaz et al. [2017] mixed the Tukey EWMA and CUSUM charts, and more recently, Haq [2021] provided another way to combine the two charts. Ajadi and Riaz [2017], Riaz et al. [2019], and Zaman et al. [2020] extended mixing the control charts to a multivariate level. We study the performance of mixing the EWMA and CUSUM charts in Section 3.

Other mixed control charts were also proposed in the literature. Khan et al. [2016], Ahmad et al. [2017], Taboran et al. [2019], Sukparungsee et al. [2020] and Aslam [2021] mixed the MA and EWMA charts. In this mix, either the MA statistic is used as input in the EWMA statistic, or inversely the EWMA values are used in the calculation of the MA statistic. Aslam et al. [2017b] mixed the DMA and the EWMA charts. Following Lu [2017], Ali and Haq [2018a], Ali and Haq [2018b] and Huang et al. [2020] mixed the GWMA and CUSUM charts for monitoring the process mean and variance. Mabude et al. [2020] developed a nonparametric scheme for the two mixed versions from GWMA and CUSUM charts. Aslam et al. [2018b] mixed the DEWMA and CUSUM charts to monitor Weibull distributed processes, while Nazir et al. [2021] mixed them under normal, heavy-tailed, and skewed process distributions. Taboran et al. [2021] designed a Tukey mixed MA and DEWMA chart. Abid et al. [2021a,b] mixed the CUSUM and HWMA charts in both possible orders.

In order to gain the advantage of robustness and efficient detection of small shifts, Abbas et al. [2020] introduced an EWMA chart under a progressive setup. In this chart, the EWMA and PM charts are integrated such that the PM chart statistic accumulates the EWMA statistics over time instead of the usual sample means. They evaluated the chart under normal and many non-normal distributions. Alevizakos et al. [2021i] noted that the derived chart statistic variance of Abbas et al. [2020] is incorrect and provided the corrected formula. Ajadi et al. [2020] investigated the robustness of this mixed-type chart, and Ali et al. [2021b,c] proposed a nonparametric version to it. Riaz et al. [2021d] proposed the use of the PM statistic as an input into the EWMA chart statistic.

To illustrate the performance of these approaches, the mixed EWMA-CUSUM, or MEC, chart from Abbas et al. [2013] is considered in Section 4. The complications of these types of compound charts do not lead to performance advantages over well-designed traditional methods.

3 Basic Definitions, ARL types and the standard competitor

For simplicity, we consider an independent series X_1, X_2, \dots following a normal distribution with mean μ and standard deviation σ . Moreover, the following change point (τ) model

$$\mu = \begin{cases} \mu_0 = 0 & , t < \tau \\ \mu_1 = \delta & , t \geq \tau \end{cases} \quad (1)$$

is applied. The standard deviation is assumed to be known, $\sigma = \sigma_0 = 1$ (otherwise normalize the X_t), and to remain constant.

We denote by L (later it becomes more explicit) the run length stopping time, which is the number of observed X_i values until an alarm is flagged. Its averages for the two situations, $\tau = 1$ and $\tau = \infty$, are referred to as the zero-state Average Run Length (ARL) values, cf. to Page [1954], Crosier [1986]. Commonly control charts are designed to exhibit a certain in-control ARL, namely $E_\infty(L) = A$ for some suitably large number A . Afterwards, specific out-of-control ARL values are determined, namely $E_1(L)$ for specified values of δ , to fill tables or to create ARL profile diagrams.

Focusing to the simple case $\tau = 1$ in (1) is often misleading. Therefore, we consider as well the conditional expected delay (CED)

$$D_\tau = E_\tau(L - \tau + 1 \mid L \geq \tau)$$

and, if appropriate, the conditional steady-state ARL

$$\mathcal{D} = \lim_{\tau \rightarrow \infty} D_\tau.$$

Note that both the sequence of CED values $\{D_\tau\}$ and the limit \mathcal{D} are functions of the shift size δ . For most of the conventional control charts, the sequence converges rapidly to \mathcal{D} . Therefore, the conditional steady-state ARL \mathcal{D} is another valuable and representative performance measure.

For the most part, we use the standard EWMA chart as our benchmark scheme, as proposed by Roberts [1959]. We use the version with exact control limits, that is, time varying ones. MacGregor and Harris [1990] acknowledged that these limits introduce some fast initial response properties. So we apply

$$Z_0 = \mu_0 = 0 \quad , \quad Z_i = (1 - \lambda)Z_{i-1} + \lambda X_i \quad , \quad i = 1, 2, \dots, \quad (2)$$

$$L_E = \min \left\{ i \geq 1 : |Z_i - \mu_0| > c_E \sqrt{(1 - (1 - \lambda)^{2i}) \frac{\lambda}{2 - \lambda}} \right\}. \quad (3)$$

In contrast to most of the schemes we review and study in our paper, numerical routines are fully established to calculate the zero-state ARL, the CED, and the steady-state ARL. Here, we utilize the R package `spc` [Knoth, 2021].

4 Mixed EWMA-CUSUM charts

After some early experiments applying runs rules to the EWMA chart [Abbas et al., 2011] and to the CUSUM chart [Riaz et al., 2011b], as discussed in the next section, these authors introduced in Abbas et al. [2013] an amalgam of the EWMA and CUSUM charts, in short the MEC chart. In particular, they consider the usual, see (2), EWMA sequence for $i = 1, 2, \dots$,

$$Q_i = (1 - \lambda_q)Q_{i-1} + \lambda_q X_i, \quad Q_0 = 0$$

and utilize Q_i instead of the original X_i as input for a CUSUM chart, namely

$$M_i^+ = \max \{0, M_{i-1}^+ + Q_i - a_i\}, \quad M_0^+ = 0,$$

$$M_i^- = \max \{0, M_{i-1}^- - Q_i - a_i\}, \quad M_0^- = 0.$$

The CUSUM's reference values are set to $a_i = a^* \sigma_{Q,i}$, where the latter symbol represents the standard deviation of the statistic Q_i , cf. to (3):

$$\sigma_{Q,i} = \sqrt{\frac{\lambda_q}{2 - \lambda_q} (1 - (1 - \lambda_q)^{2i})}. \quad (4)$$

In a similar way the alarm rule is adapted, that is,

$$L_{MEC} = \min \{i \geq 1: \max\{M_i^+, M_i^-\} > b^* \sigma_{Q,i}\}.$$

For given λ_q , a^* values and some in-control ARL level A , the threshold constant b^* is calculated by running a Monte-Carlo study. For $\lambda_q \in \{0.1, 0.25, 0.5, 0.75\}$, the out-of-control zero-state ARL for selected shifts is determined, again by performing Monte-Carlo experiments. The authors chose $a^* = 0.5$ and compared the MEC ARL profiles with the one resulting from a standard CUSUM chart configured with $k = a^*$. Recall the simple setup of the classical CUSUM:

$$C_i^+ = \max \{0, C_{i-1}^+ + X_i - k\}, C_0^+ = 0, \quad (5)$$

$$C_i^- = \max \{0, C_{i-1}^- - X_i - k\}, C_0^- = 0, \quad (6)$$

$$L_C = \min \{i \geq 1: \max\{C_i^+, C_i^-\} > h\}. \quad (7)$$

It is not surprising that MEC chart with all the considered λ_q values performs better for small shifts. Here, we propose to compare the MEC design for a given λ_q with a CUSUM chart, where the k is chosen more appropriately. By using the asymptotic standard deviation of Q_i , the limit of (4)

$$\sigma_{Q,\infty} = \lim_{i \rightarrow \infty} \sigma_{Q,i} = \sqrt{\frac{\lambda_q}{2 - \lambda_q}},$$

we set $k = a^* \sigma_{Q,\infty}$. Note that the determination of h is much simpler than that of b^* . After applying this $k = k(\lambda_q, a^*)$ rule, we obtained the reference values in Table 1. Note that the trivial choice $\lambda_q = 1$ refers

Table 1: Suitable reference values k for the ARL competition between MEC and CUSUM; alarm thresholds h for the simple CUSUM (in-control $A = 170$) are given as well.

λ_q	0.1	0.25	0.5	0.75	1
k	0.1147	0.1890	0.2887	0.3873	0.5
h	9.8345	7.7120	5.9798	4.8799	4.0133

to the simple CUSUM chart. The values h are calculated by using the function `xcusum.crit()` from the R package `spc`.

For the ARL competition, we look again at the zero-state ARL and the CED with its limit, the conditional steady-state ARL. In the following figures, we illustrate the CED profiles for two selected shifts, $\delta \in \{0.5, 1.5\}$. We start with the case $\delta = 0.5$ in Figure 1. For the considered designs, the MEC chart features a slightly

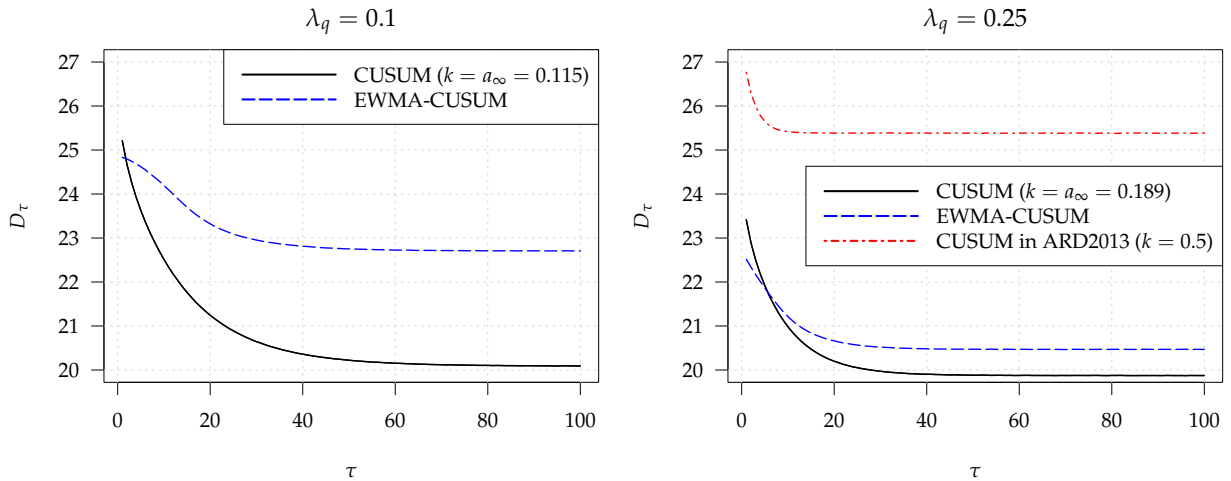


Figure 1: CED profiles, $D_\tau = E_\tau(L - \tau + 1 | L \geq \tau)$ vs. change-point position τ , for shift $\delta = 0.5$, in-control (zero-state) ARL is $A = 170$; the red dash-dotted line in the $q = 0.25$ diagram refers to the profile $k = 0.5$ utilized by Abbas et al. [2013].

better zero-state (i.e., $\tau = 1$) ARL values and slightly lower D_τ values for values of $\tau \leq 5$. However, one can conclude that the more complicated MEC scheme does not exhibit better detection performance than the CUSUM chart. Finally we observe that the reference value $k = 0.5$ (the respective profile is plotted in the $\lambda_q = 0.25$ diagram) chosen in [Abbas et al. \[2013\]](#) creates an unfair disadvantage for the family of CUSUM charts.

Turning to the larger shift, $\delta = 1.5$ in [Figure 2](#), we conclude that the MEC chart is uniformly dominated by

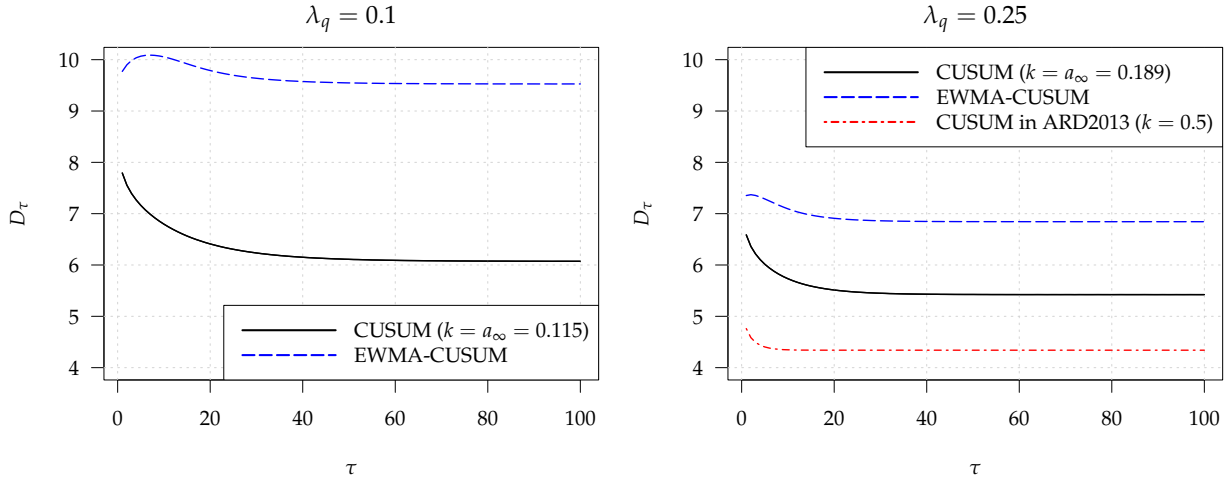


Figure 2: CED profiles, $D_\tau = E_\tau(L - \tau + 1 \mid L \geq \tau)$ vs. change-point position τ , for shift $\delta = 1.5$, in-control (zero-state) ARL is $A = 170$; the red dash-dotted line in the $q = 0.25$ diagram refers to the profile $k = 0.5$ utilized by [Abbas et al. \[2013\]](#).

the respective CUSUM chart. This is not really surprising, because for larger changes the original CUSUM chart with $k = 0.5$ performs the best.

From all profiles in [Figures 1 and 2](#) we observe that the CED converges quite quickly to the conditional steady-state ARL. Therefore, we are free to utilize the latter as a representative delay measure for roughly all change point positions.

In [Figure 3](#) we present a final ARL analysis of our two MEC designs ($\lambda_q = 0.1$ and $= 0.25$) together with their CUSUM chart opponent. Essentially, the simpler CUSUM chart exhibits better or similar ARL results compared to the MEC chart. For very small δ values, the MEC chart exhibits slightly lower out-of-control zero-state ARL results, whereas for medium size and large shifts, the CUSUM chart is substantially better. In case of the steady-state ARL, the CUSUM chart is for all shifts as least as good as the MEC chart while being much better again for medium size shifts and larger ones.

Finally we want to mention that in the case of the CUSUM chart, the zero-state ARL is equal to the worst case ARL, where [Moustakides \[1986\]](#) proved optimality (at $\delta = 2k$) for the CUSUM chart. Contrarily, for the MEC chart the worst case ARL is larger than the zero-state ARL. Refer to [Figure 4](#). The worst-case MEC ARL is more difficult to determine, because the worst case is characterized by $M_{\tau-1}^+ = 0$ and $Q_{\tau-1} \ll 0 = \mu_0$, whereas for the zero-state ARL we deploy simply $Q_0 = 0$ (change-point $\tau = 1$). We demonstrate this by considering a simplified situation. We condition on the first observation $X_1 = x_1$ and calculate the ARL for $\tau = 2$. Next, we plot these values as a function of $-4 \leq x_1 \leq 4$ (as long as $|x_1| \leq h + k$ and $\leq b^* + a^*$, it does not trigger an alarm, respectively; in all cases the right-hand sides are larger than 5). We consider three different shifts, $\delta \in \{0.5, 0.75, 1\}$. First, we recognize the constant parts of the CUSUM profiles for $x_1 \leq k$. Second, the MEC chart branches on the left-hand side reside clearly above the reported zero-state ARL (and as well above D_2). For the CUSUM chart, however, the constant part is at the zero-state ARL level. The values in [Figure 4](#) were estimated using Monte Carlo simulations. Differently from D_2 (plotted in [Figures 1 and 2](#)), the first observation X_1 is not drawn from $\mathcal{N}(0, 1)$ (the in-control model), but set to be just $X_1 = x_1$. In this way, we simulated

$$\ell(x_1) := E_2(L - 1 \mid L \geq 2, X_1 = x_1) = E_2(L - 1 \mid X_1 = x_1) \quad \text{for } -4 \leq x_1 \leq 4.$$

And of course $\sup_{-4 \leq x_1 \leq 4} \ell(x_1) = \mathcal{L}$ for the CUSUM chart. In [Figure 4](#) we observe that the respective sup for the MEC chart might be substantially larger than its zero-state ARL \mathcal{L} .

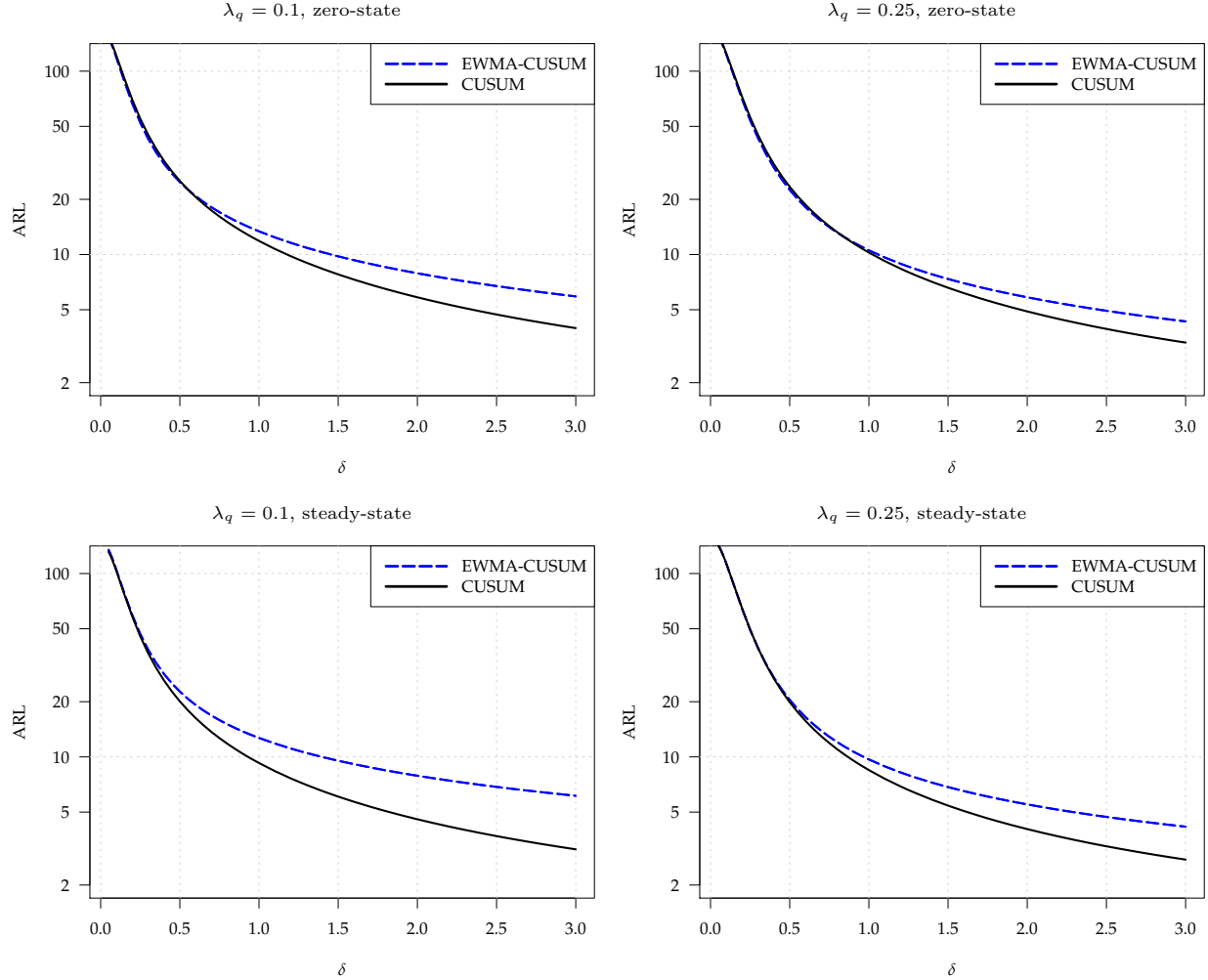


Figure 3: Zero-state and (conditional) steady-state ARL of MEC and CUSUM vs. shift size δ , in-control (zero-state) ARL is $A = 170$.

Summing up, we find that for any MEC chart design, we can find a CUSUM control chart that exhibits nearly the same zero-state ARL, lower steady-state ARL and lower worst case ARL. Thus, the larger efforts involved in setting up and using a MEC chart do not pay off. A simpler CUSUM chart does the job better with less effort.

5 Runs rule CUSUM and EWMA charts

Riaz et al. [2011b] and Abbas et al. [2011] proposed to impose on the CUSUM and EWMA charts certain runs rules. The latter are classical improvements to Shewhart type charts to introduce some memory into these simple and very popular devices. These rules were considered in Dudding and Jennett [1942] and Weiler [1953], but more familiar references are likely WECO [1956] and Nelson [1984]. Runs rules experienced some renaissance later on, see, for example, Klein [2000], Khoo [2003] and Koutras et al. [2007]. Regarding their ARL analysis we refer to Champ and Woodall [1987] and Champ [1992].

In Riaz et al. [2011b], classical 2-of-2 and 2-of-3 rules augment a standard CUSUM control chart as supplementary rules. Differently, Abbas et al. [2011] established the classical 2-of-2 and a modified 2-of-3 rule as sole alarm rule for an EWMA control chart. While the former needs alarm and warning limits (denoted with AL and WL), the latter utilizes only warning thresholds.

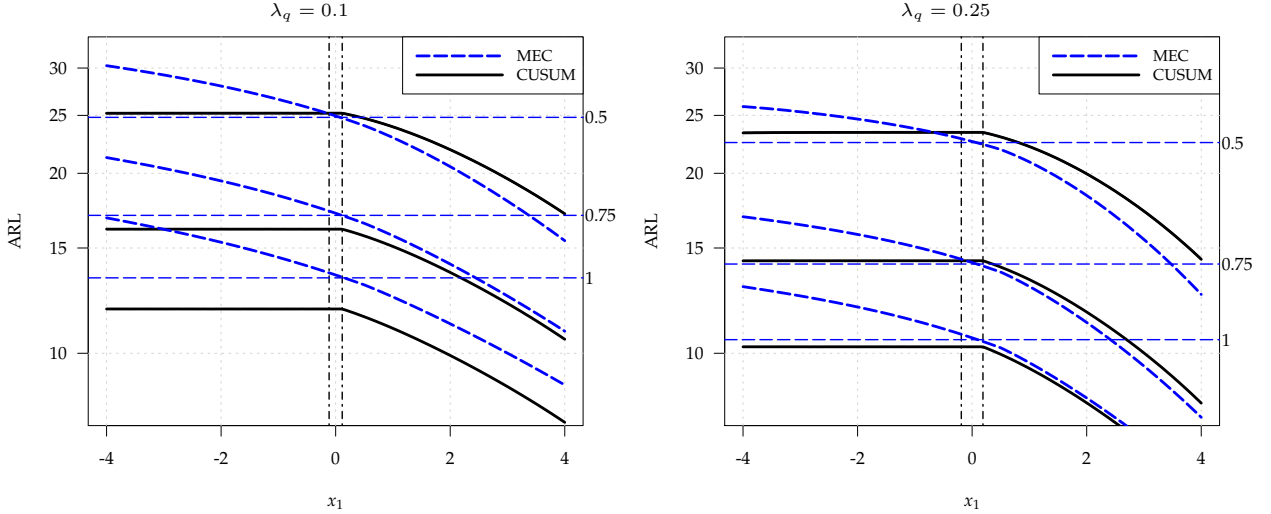


Figure 4: Effective out-of-control ARL, conditioned on first observation $X_1 = x_1$ for MEC and CUSUM; three shifts $\delta \in \{0.5, 0.75, 1\}$; MEC zero-state ARL added as horizontal lines; vertical lines are added at $(-k, k)$.

We start with the two RR-CUSUM schemes in Riaz et al. [2011b]. In both cases, an alarm is triggered if the standard CUSUM rule triggers a signal, see (7), or two of two (three) consecutive points of C_i^+ or C_i^- in (5) and (6), respectively, reside between the warning limit WL and the alarm limit $AL = h$. In both publications — cf. to the corresponding PhD thesis Abbas [2012] — the zero-state ARL was estimated using a Monte Carlo study. By utilizing the Excel Add-In MCSim [Bois and Maszle, 1997] and 5 000 replications, all the ARL estimates were determined. Unfortunately, neither in the journal publications nor in the PhD thesis was the Monte Carlo design sufficiently described in detail. As examples, we picked some results from Table II/III in Riaz et al. [2011b] and compared them to results of a more extensive Monte Carlo study with 10^8 replications in Table 2. Moreover, we provided slightly changed alarm limits, AL^* , that ensure the nominal in-control zero-state ARL of 168. Note that $AL^* = \infty$ corresponds to applying only the runs rule. Note that for all shifts $\delta \geq 0.75$ we clearly confirm the results of Riaz et al. [2011b], whereas we observe a gap between our values and theirs for the smaller shifts, $\delta = 0.25$ and $= 0.5$. Using the corrected alarm limits, AL^* , and the larger “power” of a 10^8 Monte Carlo study, we repeated the competition between the two RR-CUSUM control charts and the standard CUSUM chart. From Table 3 we conclude that the $k = 0.4933$ CUSUM chart beats all the RR-CUSUM designs. But the main result is that there is no convincing reason to abstain from using the initial $k = 0.5$ CUSUM chart, whose out-of-control ARL results are sufficiently small compared to all considered RR-CUSUM schemes.

Turning to Abbas et al. [2011] RR-EWMA schemes, we observe several particularities. As already mentioned, the runs rule is deployed standalone. Second, the 2-of-3 rule is more involved. The version for the lower limit is given by “At least two out of three consecutive points fall below an LSL and the point above the LSL (if any) falls between the CL and the LSL” [Abbas et al., 2011]. Third in Abbas et al. [2011] and as well in Abbas [2012], wrong ARL results for the modified 2-of-3 rule were reported. Later, in Abbas et al. [2015], these values were corrected. Presumably, Khoo et al. [2016] evoked these corrections by writing “While highlighting some erroneous average run length (ARL) and standard deviation of the run length (SDRL) computations in Abbas et al. (2011)”. At least, Abbas et al. [2015] explained what happened some years before: “The reason is being the omitted statement in a simulation code (mistakenly) dealing with the lower sided limit”. This means that ARL values of a one-sided scheme were reported inadvertently. This led as well to an incorrect control (alias warning) limit. Fourth, the authors compared the two RR-EWMA schemes with many other control charts, but not to the standard EWMA chart, cf. to (3). Here, see Table 4, we start with a comparison of the 2-of-2 EWMA chart with the standard EWMA chart. We match the competitors by simply using the same value for λ as done in Abbas et al. [2011]. For the standard EWMA we used 170 as nominal in-control ARL. First, we see from Table 4 that the uniformly best out-of-control ARL values are obtained for the standard EWMA chart with $\lambda = 0.1$. We observe for both EWMA schemes, that the out-of-control ARL decreases with decreasing λ . Finally, setting λ of the standard EWMA to $= 0.23$, $= 0.44$ and $= 0.61$, we obtain designs whose out-of-control ARL values are uniformly smaller than the ones of the 2-of-2 EWMA with $\lambda = 0.25$, $= 0.5$ and $= 0.75$, respectively.

Table 2: ARL results from Table II/III in Riaz et al. [2011b] augmented with new results obtained with 10^8 replications (second line).

WL	AL	δ						AL^*
		0.25	0.5	0.75	1	1.5	2	
2-of-2								
3.42	4.8	71.87	25.56	13.54	8.66	5.08	3.68	∞
		73.60	26.68	13.51	8.67	5.08	3.69	
3.44	4.6	72.26	25.65	13.50	8.57	5.01	3.61	4.65
		73.91	26.70	13.48	8.62	5.01	3.61	
3.48	4.4	71.94	25.59	13.50	8.52	4.94	3.52	4.38
		74.31	26.73	13.44	8.56	4.94	3.53	
3.53	4.2	71.40	25.30	13.33	8.40	4.83	3.42	4.23
		73.55	26.51	13.30	8.44	4.84	3.44	
2-of-3								
3.5	4.44	71.49	25.38	13.40	8.46	4.94	3.54	4.52
		73.38	26.52	13.37	8.54	4.95	3.55	
3.6	4.19	72.94	25.37	13.35	8.38	4.83	3.42	4.18
		74.13	26.61	13.33	8.46	4.84	3.44	
3.7	4.08	73.11	25.37	13.31	8.34	4.78	3.38	4.08
		74.23	26.62	13.30	8.41	4.79	3.38	
3.8	4.03	73.59	25.40	13.28	8.32	4.75	3.35	4.03
		74.29	26.64	13.29	8.39	4.76	3.36	

Finally, we consider the modified 2-of-3 EWMA chart and focus on one example, namely $\lambda = 0.1$ and target in-control ARL 168. In Table 5, we provide the incorrect numbers from Abbas et al. [2011] and the corrected ones in Abbas et al. [2015], new ones from another Monte Carlo study with 10^8 replications for the common 2-of-3 EWMA chart and results for the standard EWMA chart calculated with the R package `spc`. At the bottom line we added as well the control limit factors used. We observe again that the standard EWMA chart exhibits the lowest zero-state ARL numbers. Regarding the comparison for other values of λ , we observe a similar behavior as for the 2-of-2-EWMA discussed above. Comparing the results of Abbas et al. [2015] and the ones for the common 2-of-3 EWMA, we acknowledge their similarity. It indicates that the modified 2-of-3 rule could be reduced to the standard one, where the “point above the LSL (if any) falls between CL and the LSL” condition is dropped.

Khoo et al. [2016] provided a Markov chain approximation technique for the two RR-EWMA charts. However, there are two differences. First, they considered constant signal limits relying on the asymptotic EWMA variance $\lambda/(2 - \lambda)$. Second, they utilized the standard (they called it non-side-sensitive) 2-of-3 runs rule, where it is not important anymore, whether the “unobtrusive” EWMA value is on the right side of the center line. We dealt with this case in Table 5 already. Khoo et al. [2016] investigated further types of RR-EWMA charts, where for the most complicated one (four runs rules) it was declared “it is found that generally the four runs rules EWMA schemes outperform all charts under comparison, in terms of ARL”. However, they applied again the oversimplified approach of equalizing the λ values. If we compare the four runs rule EWMA charts with $\lambda = 0.1, 0.2, 0.3, \dots, 0.9$ to the standard EWMA chart with instead $\lambda = 0.09, 0.18, 0.26, \dots, 0.62$, respectively, then we obtain charts which exhibit lower out-of-control ARL values for all considered [in Khoo et al., 2016] shifts $\delta = 0.1, 0.2, \dots, 7$. In summary, the ad hoc use of runs rules EWMA charts is not worth the required effort.

6 MA, DMA, TMA and QMA Charts

The moving average (MA) is a well-known filtering technique for time series data. Thus, it is not surprising that it was proposed as well for doing process monitoring, but only relatively few papers have dealt with it. Roberts [1966] was presumably the first, whereas Lai [1974] provided some results for moving averages in

Table 3: Repeating the [Riaz et al. \[2011b\]](#) competition between the 2-of-2, 2-of-3 and the standard CUSUM.

WL/k	AL/h	δ					
		0.25	0.5	0.75	1	1.5	2
2-of-2							
3.42	∞	74.12	26.88	13.68	8.84	5.31	4.00
3.44	4.65	74.12	26.75	13.51	8.64	5.04	3.63
3.48	4.38	74.13	26.69	13.42	8.54	4.93	3.52
3.53	4.23	74.05	26.63	13.35	8.47	4.86	3.45
2-of-3							
3.5	4.52	73.87	26.64	13.43	8.58	4.99	3.58
3.6	4.18	73.96	26.58	13.32	8.45	4.83	3.43
3.7	4.08	74.23	26.62	13.30	8.41	4.79	3.38
3.8	4.03	74.29	26.64	13.29	8.39	4.76	3.36
standard CUSUM							
0.50	4.002	74.31	26.65	13.29	8.39	4.75	3.34
0.4933	4.045	73.86	26.48	13.25	8.39	4.76	3.36
0.49	4.067	73.64	26.40	13.23	8.39	4.77	3.37
0.48	4.134	72.96	26.16	13.18	8.39	4.80	3.39

Table 4: Table II of [\[Abbas et al., 2011\]](#) and standard EWMA ARL results.

δ	EWMA w/ and w/o runs rule							
	$\lambda = 0.1$		$\lambda = 0.25$		$\lambda = 0.5$		$\lambda = 0.75$	
0.00	169.87	169.99	169.48	169.99	169.68	169.98	169.71	170.02
0.25	54.58	53.98	73.48	74.54	94.82	99.53	110.78	118.63
0.50	19.80	18.92	26.63	26.46	37.99	41.20	49.06	58.77
0.75	10.59	9.79	12.95	12.63	17.41	19.22	23.29	29.29
1.00	6.94	6.16	7.95	7.48	9.88	10.51	13.07	15.90
1.50	4.11	3.28	4.35	3.76	4.73	4.51	5.58	6.15
2.00	2.98	2.16	3.10	2.41	3.12	2.69	3.34	3.21
L_S/c_E	2.145	2.2145	2.184	2.6282	2.034	2.7241	1.830	2.7493

general. Then [Wong et al. \[2004\]](#) provided some guidelines to apply MA control charts. Essentially, the latter authors found that the detection performance of MA charts to be quite similar to that of EWMA charts. They claimed as well that the MA principle is more popular than EWMA in several fields such as finance. However, later on [Khoo and Wong \[2008\]](#) introduced the so-called double MA (DMA) chart. It is based on the following equations with w representing the window size:

$$M_i = \begin{cases} \frac{1}{i} \sum_{j=1}^i X_j & , i \leq w \\ \frac{1}{w} \sum_{j=i-w+1}^i X_j & , i \geq w \end{cases} , \quad D_i = \begin{cases} \frac{1}{i} \sum_{j=1}^i M_j & , i \leq w \\ \frac{1}{w} \sum_{j=i-w+1}^i M_j & , i \geq w \end{cases} .$$

Beginning with $i \geq w$, the ordinary MA statistics M_i sum the most recent w observations with equal weight $1/w$. In contrast, the double MA statistic involves more data points. Namely starting with $i \geq 2w - 1$ it sums the most recent $2w - 1$ observations with triangular weights $1/w^2, 2/w^2, \dots, (w-1)/w^2, w/w^2, (w-1)/w^2, \dots, 1/w^2$. Obviously, the data point in the middle of the window is given the same weight as the ones in the MA sum, whereas the others get smaller weights. Straightforwardly, [Khoo and Wong \[2008\]](#) proposed the control limits $\mu_0 \pm L\sqrt{Var(D_i)}$. However, they made a mistake while calculating the variance term. [Alevizakos et al. \[2020\]](#) spotted it and provided correct formulas. Here, we want to consider only the case

Table 5: Zero-state ARL values for modified 2-of-3 EWMA from Table III of [Abbas et al. \[2011\]](#), [Abbas et al. \[2015\]](#) and a further Monte Carlo study for the common 2-of-3 EWMA, and for standard EWMA (R package `spc`); $\lambda = 0.1$.

	modified 2-of-3		2-of-3	standard
δ	(2011)	(2015)	10^8	<code>spc</code>
0.00	167.32	167.09	<i>166.36</i>	168.00
0.25	34.37	53.71	<i>53.70</i>	53.59
0.50	14.04	19.37	<i>19.40</i>	18.83
0.75	8.13	10.40	<i>10.42</i>	9.75
1.00	5.71	6.83	<i>6.84</i>	6.14
1.50	3.78	4.01	<i>4.02</i>	3.27
2.00	3.20	2.96	<i>2.96</i>	2.15
L_S/c_E	1.807	2.158	2.158	2.4098

$i \geq 2w - 1$, where [Khoo and Wong \[2008\]](#) gave an overly simple result. We have

$$\text{Var}(D_i) = \begin{cases} \frac{1}{w^2} & , \text{Khoo and Wong [2008]}, \\ \frac{1}{w^2} \left[1 + \frac{2}{w^2} \sum_{w \leq j_1 < j_2 \leq 2w-1} (j_1 - j_2 + w) \right] & , \text{Alevizakos et al. [2020]}, \\ \frac{1}{w^2} \left[1 + \frac{2}{w^2} \sum_{j=1}^{w-1} j^2 \right] = \frac{1}{w^2} \left[1 + \frac{(w-1)(2w-1)}{3w} \right] & , \text{summing squared weights.} \end{cases}$$

Some tedious algebra shows that the two last two expressions are equivalent. [Alevizakos et al. \[2020\]](#) provided a few comparisons between MA, DMA, EWMA and CUSUM charts. Unfortunately, the opponents are chosen in either an unfair (take the same w for MA and DMA charts) or in an arbitrary way with EWMA and CUSUM charts. Here, we match MA(w_1), DMA(w_2) and EWMA(λ), aiming at roughly the same final variance of the plotted statistic. Thus, starting with some w_2 for the DMA chart, we determine

$$\sigma_D^2 = \frac{1}{w_2^2} \left[1 + \frac{(w_2-1)(2w_2-1)}{3w_2} \right], \quad w_1 = \left\lceil \frac{1}{\sigma_D^2} \right\rceil, \quad \lambda = \frac{2\sigma_D^2}{\sigma_D^2 + 1}.$$

Here $\lceil \cdot \rceil$ denotes rounding to the next integer.

Now we re-arrange some zero-state ARL results from Tables 3 and 4 in [Alevizakos et al. \[2020\]](#) in blocks in Table 6. Additional values (for $w_2 = 6$ and for $w_1 \in \{6, 7, 9\}$) were estimated with Monte-Carlo simulations (10^7 replications). The EWMA chart values were determined with the R package `spc`. To make comparisons between the MA and DMA charts easy (EWMA is left out for the moment), we bolded the smaller ARL per block and δ . From the results we conclude that the simpler and older MA chart performs for the most part better than the DMA chart.

[Wong et al. \[2004\]](#) stated: “For zero state [ARL], it was found that among all MA charts (with different values of w) with the same in-control ARL, the chart with the largest w is always the quickest in detecting any finite shift. In other words, no optimal chart within the class of MA charts can be found.” Similar patterns could be observed for the DMA chart [slight deviations in Table 3 of [Alevizakos et al., 2020](#), are probably Monte Carlo artefacts]. To avoid arbitrariness, one has to move away from the zero-state ARL competition. For instance, [Wong et al. \[2004\]](#) followed an old design principle, “the steady state run length will be considered”, which we apply here as well considering the CED. Here, we pick the configurations from the last block of Table 6 and determine $\{D_\tau\}_{\tau=1}^{100}$, see Figure 5. The results for the MA and DMA charts were obtained again by Monte Carlo simulations (10^7 replications), whereas the EWMA values were calculated with `xewma.arl()` from the R package `spc`. The CED profiles of the three control charts mirror the ordering of the corresponding zero-state ARL results. We can briefly summarize the four diagrams in Figure 5 with two statements. It is easy to find a MA control chart which performs overall better than any given DMA control chart. Second, the steady-state ARL of the DMA chart could be substantially larger than the zero-state ARL (see $\delta = 2$ and $= 3$).

To complete this steady-state ARL comparison, we utilize D_{100} as proxy (motivated by the stable convergence patterns in Figure 5) and conduct an investigation concerning setups minimizing the steady-state ARL for a

Table 6: Zero-state ARL of DMA(w_2), MA(w_1), and EWMA(λ); nominal in-control ARL of 370.

	δ									
	0	0.2	0.4	0.6	0.8	1.0	1.25	1.5	2	3
$w_2 = 2$	371.5	250.2	119.4	57.7	29.7	17.4	9.7	6.3	3.4	1.7
$w_1 = 3$	369.8	244.7	109.4	51.1	26.4	15.4	8.8	5.7	3.1	1.6
$\lambda = 0.545$	370.0	246.0	114.0	54.0	28.3	16.4	9.4	6.1	3.3	1.6
$w_2 = 3$	370.3	218.0	90.5	40.8	21.6	12.9	7.7	5.4	3.3	1.7
$w_1 = 4$	370.5	222.4	92.0	42.3	21.5	12.6	7.3	4.9	2.8	1.6
$\lambda = 0.380$	370.0	212.0	84.5	37.8	19.8	11.9	7.3	5.0	3.0	1.6
$w_2 = 4$	369.6	198.9	75.3	33.6	18.1	10.9	7.1	5.1	3.3	1.6
$w_1 = 6$	370.8	193.8	71.8	31.4	16.5	10.0	6.3	4.4	2.7	1.5
$\lambda = 0.293$	370.0	189.7	69.5	30.6	16.4	10.2	6.5	4.6	2.8	1.6
$w_2 = 5$	369.7	186.0	65.5	29.6	15.9	10.2	7.0	5.2	3.3	1.6
$w_1 = 7$	370.8	183.2	65.5	28.6	15.2	9.4	6.0	4.3	2.7	1.5
$\lambda = 0.239$	370.0	173.6	60.5	26.7	14.6	9.3	6.1	4.4	2.8	1.6
$w_2 = 6$	370.6	172.4	60.0	26.8	15.0	9.9	6.9	5.2	3.2	1.5
$w_1 = 9$	370.4	166.7	56.6	24.8	13.6	8.6	5.7	4.1	2.6	1.5
$\lambda = 0.202$	370.0	161.4	54.4	24.3	13.6	8.8	5.9	4.3	2.7	1.5

given shift, the results are given in Figure 6. For the MA and DMA charts, we picked values w up to 80 and 60, respectively, and estimated the CED at $\tau = 100$, namely D_{100} , by using a Monte Carlo simulations with 10^7 replications. From the resulting profiles (D_{100} vs. w) we observe a couple of facts. Only for $\delta = 0.2$ (which is a more of an academic choice) and to lesser extent for $\delta = 0.4$, the optimum w values are substantially large. Second, the DMA curves increase more profoundly than for the MA chart in case of medium and large shifts. This signals trouble for these shifts if one aims at optimizing the DMA chart for small shifts. It should be noted that all MA minima are smaller than their DMA counterparts. Thus, if one is interested in minimizing the steady-state ARL at a single shift δ , then the MA chart will beat the DMA chart for all settings we considered. The optimal choices of w for the MA and DMA charts are marked and collected in the Table 7 together with the respective λ values of the EWMA chart. From these configurations, we select the ones for $\delta = 0.6$ and $\delta = 1.5$ to demonstrate the steady-state ARL behavior over a range of shifts. The

Table 7: Optimal (to minimize D_{100}) choices of w and λ for MA, DMA and EMWA; in-control ARL is 370.

δ	0.2	0.4	0.6	0.8	1	1.25	1.5	1.75	2	2.5	3
w_1	76	35	20	13	9	7	5	4	3	2	2
w_2	44	22	12	8	6	4	3	3	2	2	2
λ	0.02	0.04	0.07	0.10	0.14	0.20	0.26	0.32	0.38	0.53	0.69

two EWMA values, 0.07 and 0.26, are quite common choices (note that for all calculations we used three digits, that is, the actual $\lambda = 0.069$ and $= 0.255$). The same is true for the MA chart [$w_1 = 20$ and $= 5$ Wong et al., 2004, considered values up to $w_1 = 30$] and DMA [$w_2 = 12$ and $= 4$ Wong et al., 2004, dealt with values up to $w_2 = 15$]. For these two settings, we determined the steady-state ARL (again using D_{100} and Monte Carlo simulation, except for the EWMA chart). The resulting profiles are given in Figure 7. The three schemes are clearly ordered. For all shifts δ , the EWMA chart is the best and the MA chart is the second best scheme. In particular for the $\delta = 0.6$ designs, the three curves clearly begin to diverge for increasing values of δ . Given the specific weighting patterns of the DMA chart, this is not surprising.

In summary, the DMA control chart design should not be used. This statement is valid as well for the even more complex triple MA [Alevizakos et al., 2021e] and quadruple MA [Alevizakos et al., 2021f] charts. Note that the computation of the variance of the respective statistics is a voluminous task resulting in various theorems in Alevizakos et al. [2021e,f]. That is, we obtain complex charts with demanding setup procedures and cumbersome Monte Carlo studies to evaluate these schemes. All three charts, DMA, TMA and QMA, exhibit the undesirable weighting pattern that the highest weight is set into the center of their respective windows, whereas the most recent data values get very low weights. This delays the detection of changes that happen later than instantly at the startup.

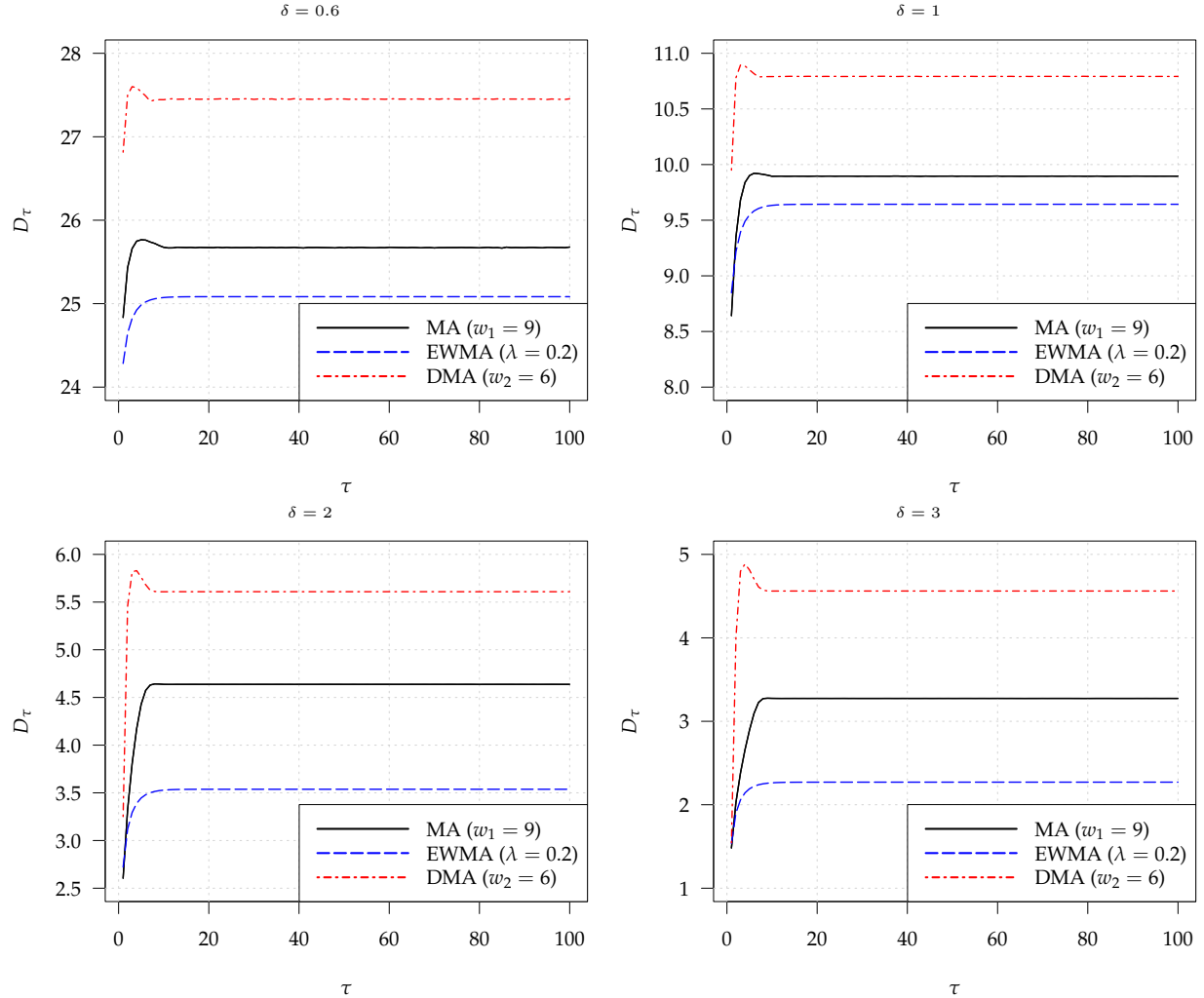


Figure 5: CED profiles of $DMA(w_2)$, $MA(w_1)$, and $EWMA(\lambda)$, i. e. $D_\tau = E_\tau(L - \tau + 1 \mid L \geq \tau)$ vs. change-point position τ , for four shifts δ ; in-control (zero-state) ARL is $A = 370$.

7 DEWMA and TEWMA Charts

The first use of two EWMA statistic iterations were proposed by [Shamma et al. \[1991\]](#) and [Shamma and Shamma \[1992\]](#). However, they did not made such an impact as the later equivalent proposals by [Zhang et al. \[2003b\]](#) and [Zhang and Chen \[2005\]](#). The more recent papers focused on the simpler case, where the smoothing constants of both EWMA series are the same, whereas the previous publications dealt with the more general case. Despite the critical statements regarding double EWMA (DEWMA) control charts in [Mahmoud and Woodall \[2010\]](#), DEWMA charts gained quite some popularity in the SPM literature. Therefore it is time to clarify in a different way that DEWMA charts are inferior to the simpler EWMA charts.

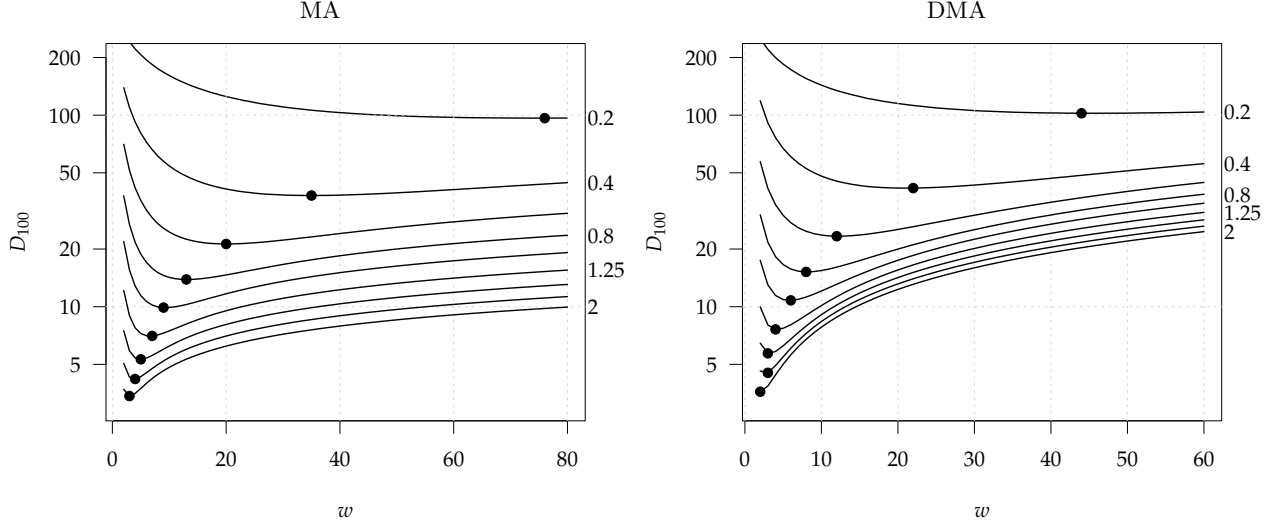


Figure 6: D_{100} profiles of MA and DMA vs. w for various shifts $\delta \in \{0.2, 0.4, \dots, 2\}$, optimal choice w per shift marked with \bullet ; in-control (zero-state) ARL is $A = 370$.

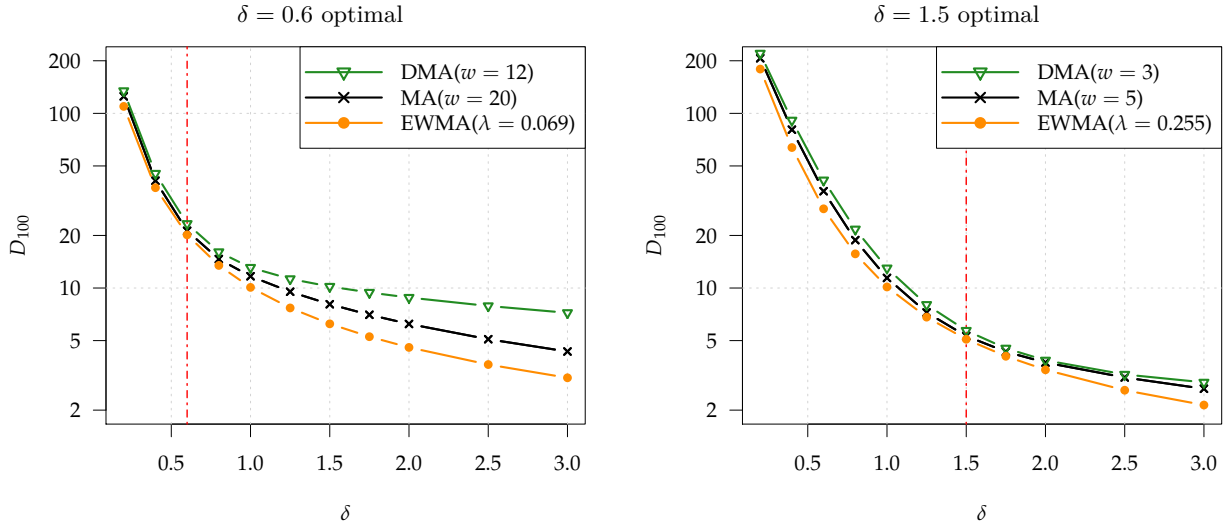


Figure 7: Steady-state ARL (D_{100}) profiles of MA, DMA and EWMA vs. δ ; in-control (zero-state) ARL is $A = 370$.

To begin, we introduce some notation. Note that we deal with the more popular case, where both EWMA equations are based on the same λ . Then, writing $\bar{\lambda} := 1 - \lambda$, we have the following equations:

$$\begin{aligned}
 Z_0^{(1)} &= \mu_0, \quad Z_0^{(2)} = \mu_0. \\
 Z_i^{(1)} &= (1 - \lambda)Z_{i-1}^{(1)} + \lambda X_i, \\
 Z_i^{(2)} &= (1 - \lambda)Z_{i-1}^{(2)} + \lambda Z_i^{(1)} \\
 &= \lambda^2 \sum_{j=1}^i (i - j + 1) \bar{\lambda}^{i-j} X_j + i \lambda \bar{\lambda}^i Z_0^{(1)} + \bar{\lambda}^i Z_0^{(2)}.
 \end{aligned}$$

From the above publications, we obtain for the variance of $Z_t^{(2)}$

$$\sigma_i^2 = \lambda^4 \frac{1 + \bar{\lambda}^2 - (i^2 + 2i + 1)\bar{\lambda}^{2i} + (2i^2 + 2i - 1)\bar{\lambda}^{2i+2} - i^2\bar{\lambda}^{2i+4}}{(1 - \bar{\lambda}^2)^3}, \quad (8)$$

$$\sigma_\infty^2 = \lambda^4 \frac{1 + \bar{\lambda}^2}{(1 - \bar{\lambda}^2)^3}. \quad (9)$$

Then by using (8), the run-length of the DWMA chart is

$$L_{DE} = \min \left\{ i \geq 1 : |Z_i^{(2)} - \mu_0| > c_{DE}\sigma_i \right\}.$$

Obviously, setup, deployment and analysis of the DEWMA chart is more complicated than for the EWMA chart. Monte Carlo analyses are required. For the EWMA chart and DEWMA chart competition, [Zhang and Chen \[2005\]](#) (and many others) picked the same λ for the EWMA chart as for the DEWMA chart. This rather oversimplified and inappropriate approach is omnipresent in the literature, unfortunately. [Mahmoud and Woodall \[2010\]](#) went a different way. They proposed to set the EWMA chart λ in such a way that for a given DEWMA design the weighting patterns of both competing charts feature the same maximum value. Here, we again aim at the same asymptotic variance, that is, choose λ_E so that $\lambda_E/(2 - \lambda_E)$ is equal to the respective DEWMA value in (9). For example, starting with DEWMA ($\lambda = 0.1$) we get (roughly) to EWMA ($\lambda = 0.05$). [Mahmoud and Woodall \[2010\]](#) determined the smaller 0.03874 EWMA smoothing constant. It turns out that aiming at equal asymptotic variances leads to larger values of λ than aiming at equal maximum weights. We will see in a moment that the slightly smaller change yields competitive EWMA designs with respect to the zero-state ARL.

Next, we present in Table 8 some results of Table 4 in [Zhang and Chen \[2005\]](#) for an in-control ARL value

Table 8: Fragments of Table 4 in [Zhang and Chen \[2005\]](#) and some more accurate numbers (labelled 10^8 and spc); zero-state ARL of DEWMA (upper block) and EWMA (lower block); in-control ARL 200.

	shift $\delta/\sqrt{5}$									
	0	0.1	0.2	0.3	0.4	0.5	1	1.5	2	
ZC2005	200.0	57.5	20.1	10.7	6.8	4.7	1.6	1.1	1.0	$\lambda = 0.1$
10^8	199.9	57.3	20.4	10.7	6.7	4.7	1.6	1.1	1.0	$\lambda = 0.1$
ZC2005	200.1	69.2	24.0	12.4	7.8	5.4	1.9	1.2	1.0	$\lambda = 0.1$
ZC2005	200.2	57.5	20.2	10.7	6.9	4.8	1.7	1.1	1.0	$\lambda = 0.05$
spc	200.0	56.9	20.4	10.7	6.8	4.8	1.7	1.1	1.0	$\lambda = 0.05$

of 200. [Zhang and Chen \[2005\]](#) compared the $\lambda = 0.1$ results, for example, and concluded “*The DEWMA mean chart performs better than the EWMA mean chart when the process mean shifts are smaller than one half of the process standard deviation*”. Of course, EWMA ($\lambda = 0.1$) exhibits larger zero-state ARL values for roughly all considered shifts. Doing the comparison, however, more appropriately, we compare with the EWMA chart with $\lambda = 0.05$ and see from Table 8 that the zero-state ARL values are roughly the same as the DEWMA chart values in the top part of the table. It remains unclear, why [Zhang and Chen \[2005\]](#) did not spot this fact.

Knowing that further decreasing the value of λ we would achieve even better zero-state ARL values of the EWMA chart for all shifts, we turn to more important properties such as CED and conditional steady-state ARL. Taking again the pair DEWMA ($\lambda = 0.1$) and EWMA ($\lambda = 0.05$), we calculated the CED for all instances in Table 8 and provide the resulting curves for four shifts in Figure 8. From the curves in Figure 8 we learn that the zero-state ($\tau = 1$) values are roughly equal as we know from Table 8, whereas for later changes the EWMA chart always exhibits lower CED values. The larger the shift, the more pronounced is the difference. For both control charts, the CED series stabilizes sufficiently quick so that we could use D_{100} as the conditional steady-state ARL and as representative delay for changes after $\tau = 30$. Next we present the resulting values in Table 9. Note that we added results for triple EWMA (TEWMA) following [Alevizakos et al. \[2021a\]](#), all calculated with 10^8 replications, smoothing constant $\lambda = 0.13$ (to achieve the same asymptotic variance as DEWMA with $\lambda = 0.1$), and a control limit factor $L = 1.91$ (in-control ARL 200). For details regarding the exact variance etc., we refer to [Alevizakos et al. \[2021a\]](#). Given the steady-state ARL results, we conclude that the EWMA chart easily dominates the DEWMA chart. From the weighting patterns in [Knoth et al. \[2021a\]](#) for the DEWMA chart (and TEWMA) we would expect this steady-state

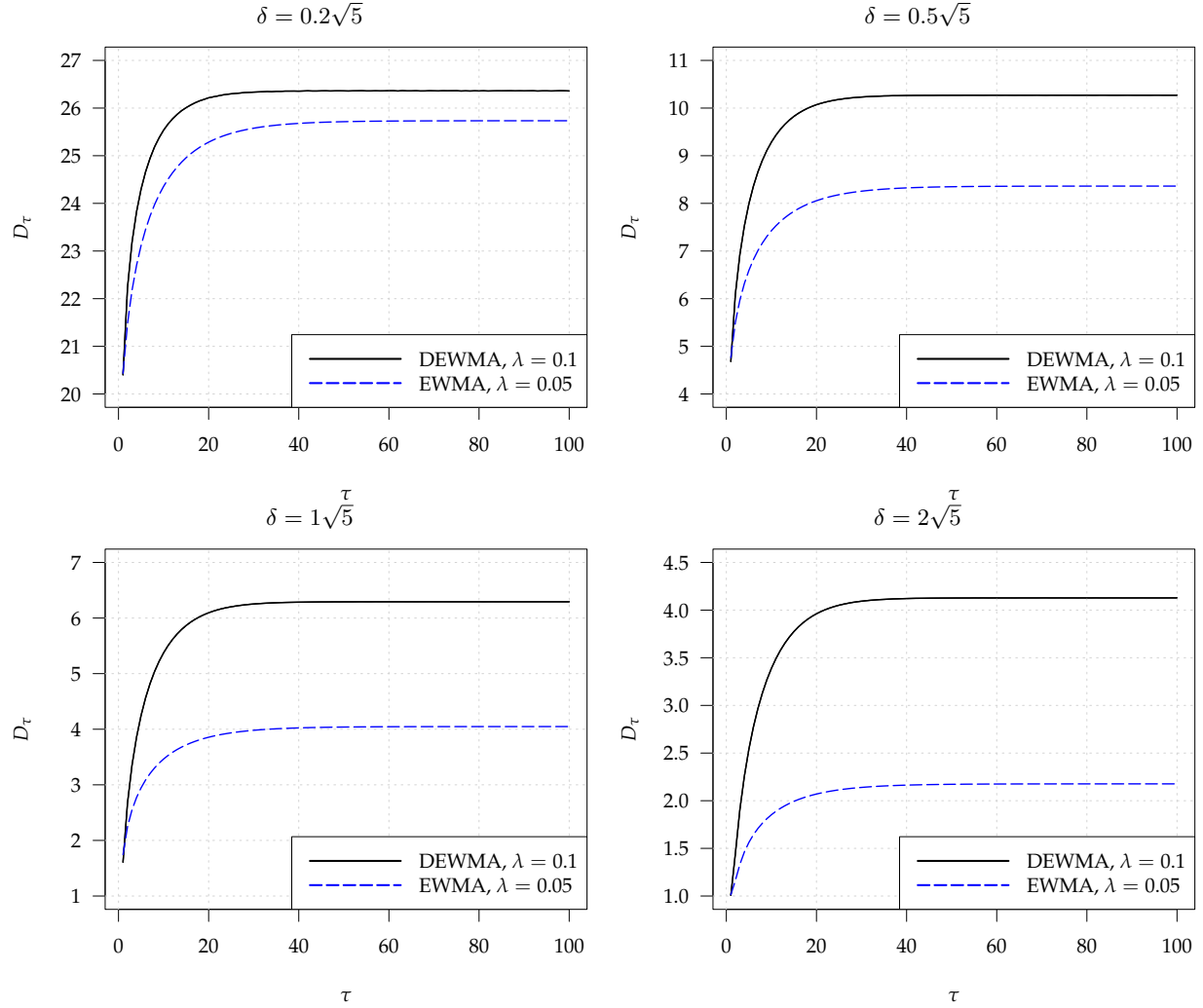


Figure 8: CED profiles of DEWMA ($\lambda = 0.1$) and EWMA ($\lambda = 0.05$), i. e. $D_\tau = E_\tau(L - \tau + 1 \mid L \geq \tau)$ vs. change-point position τ , for four shifts δ ; in-control (zero-state) ARL is $A = 200$.

Table 9: Augmenting Table 4 in Zhang and Chen [2005] with some steady-state ARL results, for DEWMA with Monte Carlo simulation (10^8 replicates) and for EWMA with the R package `spc`; in-control ARL 200; TEWMA (10^7 replicates) numbers are added too.

		shift $\delta/\sqrt{5}$								
	0	0.1	0.2	0.3	0.4	0.5	1	1.5	2	
TEWMA	-	67.4	27.9	18.3	14.6	12.6	8.5	7.0	6.1	$\lambda = 0.13$
DEWMA	-	66.1	26.4	16.4	12.4	10.3	6.3	4.9	4.1	$\lambda = 0.1$
EWMA	-	64.6	25.7	15.3	10.8	8.4	4.0	2.8	2.2	$\lambda = 0.05$

ARL deficiency. Summing up, the DEWMA (and even more the TEWMA) control chart designs are not worth the required effort. It is easy to find an EWMA design which features about the same zero-state ARL values and much better steady-state ARL results. From Mahmoud and Woodall [2010] we know that the EWMA chart exhibits better (lower) worst-case ARL results as well.

8 DPM Charts

Abbas et al. [2012] introduced the progressive mean (PM) chart. Afterwards, dozens of derivatives appeared. In Knoth et al. [2021a] it was demonstrated that the PM is not an appropriate control chart design. However, in Abbas et al. [2019] similarly to the (D)EWMA and (D)MA charts, the double PM (DPM) chart was proposed. Later, in Riaz et al. [2021a] the variance term used for constructing the alarm rule was corrected. Following the more recent paper, we describe the DPM design as follows.

$$\text{PM statistic: } P_t = \frac{1}{t} \sum_{i=1}^t X_i,$$

$$\text{DPM statistic: } D_t = \frac{1}{t} \sum_{i=1}^t P_i.$$

$$\text{PM run-length: } L_P = \min \left\{ t \geq 1: |P_t - \mu_0| > (L_P/t^{0.5})/t^p \right\},$$

$$\text{DPM run-length: } L_D = \min \left\{ t \geq 1: |D_t - \mu_0| > (L_D \sigma_{D;t})/t^p \right\}.$$

The exponent p of the curve bending factor $1/t^p$ was set to $p = 0.2$ in Abbas et al. [2012]. However, in Riaz et al. [2021a] p was taken from $\{0.35, 0.40, 0.45, 0.50\}$ (for PM and DPM). The variance of P_t is just $1/t$ which explains the $t^{0.5}$ above in L_P . The variance of DPM's D_t is much more complicated. As mentioned, Riaz et al. [2021a] corrected the old term in Abbas et al. [2019] and provided the following term

$$\sigma_{D;t}^2 = \frac{1}{t^2} \left\{ \sum_{k=1}^t \left(\sum_{j=k}^t \frac{1}{j} \right)^2 \right\} = (2t - H_t)/t^2$$

with the harmonic number $H_t = \sum_{k=1}^t 1/k$. The above simplification follows from some well-known identities for the partial sums of H_t and H_t^2 and, of course, tedious algebra. By using its approximation

$$H_t = \ln t + \gamma + \frac{1}{2t} - \frac{1}{12t^2} + \mathcal{O}\left(\frac{1}{t^4}\right)$$

the term used for $\sigma_{D;t}$ is just

$$\sigma_{D;t}^2 \approx \left(2t - \ln t - \gamma - 1/(2t) + 1/(12t^2) \right) / t^2$$

with the Euler-Mascheroni constant $\gamma = 0.57721\ 56649\ 01532\dots$. Note that this approximation is excellent. However, these mathematical developments can distract one from the actual problems with the DPM approach.

For an in-control ARL of 200, we pick $L_P = 6.415$ and $L_D = 2.596$ from Table 1 and 2 in Riaz et al. [2021a]. “Our” competitor is an EWMA chart with $\lambda = 0.05$. First, we present in Table 10 some zero-state ARL results taken from Riaz et al. [2021a], new ones with more replications (10^8) and EWMA results by deploying the R package `spc`. Riaz et al. [2021a] concluded from a graphical counterpart of our Table 10 that it “is

Table 10: Zero-state ARL numbers from Table 1 and 2 in Riaz et al. [2021a], $p = 0.35$; EWMA₁ with $\lambda = 0.05$ as common design and EWMA₂ ($\lambda = 0.007$) as a special one; in-control ARL 200.

	shift δ							
	0	0.25	0.35	0.5	0.75	1	1.5	2
PM	198.26	47.14	32.03	21.39	13.39	9.74	6.25	4.57
10^8	197.86	46.80	32.09	21.40	13.52	9.78	6.24	4.58
DPM	201.43	31.90	21.55	13.70	8.05	5.46	3.22	2.23
10^8	197.50	31.65	21.40	13.69	8.02	5.46	3.20	2.23
EWMA ₁	200.00	48.82	29.83	17.15	8.99	5.68	3.04	2.02
EWMA ₂	200.00	30.01	18.43	10.77	5.82	3.80	2.17	1.54

obvious from these graphical displays that the DPM chart takes an edge over EWMA, DEWMA, PM, HWMA, and DHWMA chart”. From Table 10 we can see, however, that this is an incorrect statement because one

could simply decrease the λ value to beat the DPM chart uniformly. However, for PM, DPM and EWMA charts with variance adjusted limits (the one we apply here), we have to consider the CED series and, if applicable, its limit. From the shifts in Table 10 we consider $\delta \in \{0.35, 0.75, 1, 2\}$ and change-point positions up to $\tau = 100$ (in-control ARL 200). In addition to Table 10, we present results as well in Figure 9 for $p = 0.2$ and $= 0.5$ in order to illustrate the impact of tuning p . Essentially, decreasing p leads to decreased zero-state ARL, while for late changes the ordering is reversed. The $p = 0.35$ curves of the PM and DPM charts are bold lines. From all four cases we conclude straightforwardly that for $\tau \geq 30$ the CED D_τ of the DPM chart

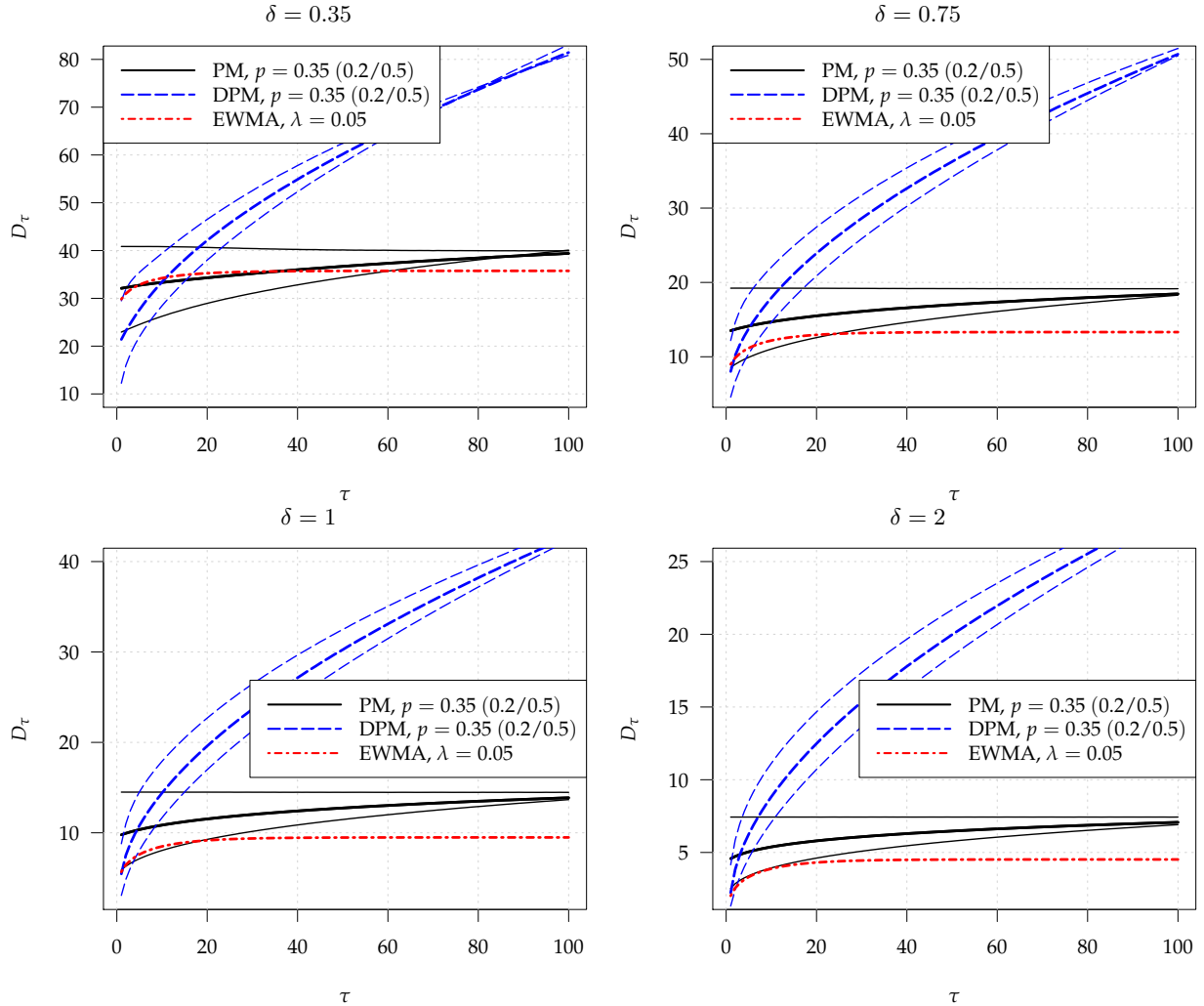


Figure 9: CED profiles of PM, DPM and EWMA ($\lambda = 0.05$), i. e. $D_\tau = E_\tau(L - \tau + 1 \mid L \geq \tau)$ vs. change-point position τ , for four shifts δ ; in-control (zero-state) ARL is $A = 200$.

is substantially larger than of the PM and EWMA charts. Even more, the DPM control chart is not able to detect delayed changes — it is not too presumptuous to conjecture that DPM’s CED series grows in an unbounded way. Only for $\tau \leq 5$ (roughly zero-state) it is usable at all. In Knoth et al. [2021a] the authors showed that the PM chart is not a good choice. From Figure 9 we can see that the DPM chart is even worse.

9 Conclusions

We find the lines of research on compound charts outlined in our paper to be misguided. It is very important for any monitoring method, for example, to be based on a weighting scheme that emphasizes the present data values more than the past data values. This rules out use of the DEWMA, triple EWMA, double MA, triple MA, quadruple MA and double PM charts. In addition, PM and HWMA charts should not be used based

on their poor steady-state run length performance. The extra complications of the GWMA chart are not justified by any improved performance relative to the simpler EWMA chart. Overall the added complexity of the various proposed compound methods is not justified by improved performance.

There is an implicit assumption in the literature reviewed here that any shift in the process, however small, is to be detected as quickly as possible. In an increasing number of applications the focus should be on detecting changes of practical importance, not just those resulting in statistical significance. More information can be found in [Woodall and Faltin \[2019\]](#).

References

- Sven Knoth, Víctor G. Tercero-Gómez, Marzieh Khakifirooz, and William H. Woodall. The impracticality of homogeneously weighted moving average and progressive mean control chart approaches. *Quality and Reliability Engineering International*, 2021a. doi:[10.1002/qre.2950](#).
- Sven Knoth, William H Woodall, and Víctor G Tercero-Gómez. The case against generally weighted moving average (GWMA) control charts. *arXiv preprint arXiv:2107.00224*, <https://arxiv.org/abs/2107.00224>, 2021b.
- James M. Lucas. Combined Shewhart-CUSUM quality control schemes. *Journal of Quality Technology*, 14(2):51–59, 1982. doi:[10.1080/00224065.1982.11978790](#).
- Muhammad Riaz, Nasir Abbas, and Ronald JMM Does. Improving the performance of CUSUM charts. *Quality and Reliability Engineering International*, 27(4):415–424, 2011a.
- Nasir Abbas, Muhammad Riaz, and Ronald J. M. M. Does. Enhancing the performance of EWMA charts. *Quality and Reliability Engineering International*, 27(6):821–833, 2011. doi:[10.1002/qre.1175](#).
- Nasir Abbas, Muhammad Riaz, and Ronald J. M. M. Does. Enhancing the performance of exponentially weighted moving average charts: discussion. *Quality and Reliability Engineering International*, 31(4):721–722, 2015. doi:[10.1002/qre.1615](#).
- Nasir Abbas, Muhammad Riaz, and Ronald JMM Does. Mixed exponentially weighted moving average–cumulative sum charts for process monitoring. *Quality and Reliability Engineering International*, 29(3):345–356, 2013. doi:[10.1002/qre.1385](#).
- Michael B. C. Khoo and V. H. Wong. A double moving average control chart. *Communications in Statistics – Simulation and Computation*, 37(8):1696–1708, 2008. doi:[10.1080/03610910701832459](#).
- S. E. Shamma, Raid W. Amin, and A. K. Shamma. A double exponentially weighted moving average control procedure with variable sampling intervals. *Communications in Statistics – Simulation and Computation*, 20(2-3):511–528, 1991. doi:[10.1080/03610919108812969](#).
- Shawky E. Shamma and Amal K. Shamma. Development and evaluation of control charts using double exponentially weighted moving averages. *International Journal of Quality & Reliability Management*, 9(6):18–25, 1992. doi:[10.1108/02656719210018570](#).
- Zameer Abbas, Hafiz Zafar Nazir, Noureen Akhtar, Muhammad Riaz, and Muhammad Abid. An enhanced approach for the progressive mean control charts. *Quality and Reliability Engineering International*, 35(4):1046–1060, 2019. doi:[10.1002/qre.2444](#).
- Vasileios Alevizakos, Kashinath Chatterjee, and Christos Koukouvinos. The triple exponentially weighted moving average control chart. *Quality Technology & Quantitative Management*, 18(3):326–354, 2021a. doi:[10.1080/16843703.2020.1809063](#).
- Abdul Haq. A new hybrid exponentially weighted moving average control chart for monitoring process mean. *Quality and Reliability Engineering International*, 29(7):1015–1025, 2013.
- Abdul Haq. A new hybrid exponentially weighted moving average control chart for monitoring process mean: Discussion. *Quality and Reliability Engineering International*, 33(7):1629–1631, 2017.
- Tze Leung Lai. Control charts based on weighted sums. *Ann. Stat.*, 2(1):134–147, 1974. doi:[10.1214/aos/1176342619](#).
- Mahmoud A. Mahmoud and William H. Woodall. An evaluation of the double exponentially weighted moving average control chart. *Communications in Statistics – Simulation and Computation*, 39(5):933–949, 2010. doi:[10.1080/03610911003663907](#).
- Lingyun Zhang and Gemai Chen. An extended EWMA mean chart. *Quality Technology & Quantitative Management*, 2(2):39–52, 2005.

- Saad Saeed Alkahtani. Robustness of DEWMA versus EWMA control charts to non-normal processes. *Journal of Modern Applied Statistical Methods*, 12(1):148–163, 2013. doi:[10.22237/jmasm/1367381820](https://doi.org/10.22237/jmasm/1367381820).
- Muhammad Shujaat Nawaz, Muhammad Azam, and Muhammad Aslam. EWMA and DEWMA repetitive control charts under non-normal processes. *Journal of Applied Statistics*, 48(1):4–40, 2021.
- Ishaq Adeyanju Raji, Nasir Abbas, and Muhammad Riaz. On designing a robust double exponentially weighted moving average control chart for process monitoring. *Transactions of the Institute of Measurement and Control*, 40(15):4253–4265, 2018.
- Azaz Ahmed, Aamir Sanaullah, and Muhammad Hanif. A robust alternate to the HEWMA control chart under non-normality. *Quality Technology & Quantitative Management*, 17(4):423–447, 2020.
- Rafael Perez Abreu and Jay R Schaffer. A double EWMA control chart for the individuals based on a linear prediction. *Journal of Modern Applied Statistical Methods*, 16(2):443–457, 2017. doi:[10.22237/jmasm/1509495840](https://doi.org/10.22237/jmasm/1509495840).
- Faiza Asif, Shahana Khan, and Muhammad Noor-ul Amin. Hybrid exponentially weighted moving average control chart with measurement error. *Iranian Journal of Science and Technology, Transactions A: Science*, 44:801–811, 2020.
- Surria Noor, Muhammad Noor-ul Amin, Muhammad Mohsin, and Azaz Ahmed. Hybrid exponentially weighted moving average control chart using bayesian approach. *Communications in Statistics – Theory and Methods*, 2020. doi:[10.1080/03610926.2020.1805765](https://doi.org/10.1080/03610926.2020.1805765).
- Muhammad Noor-ul Amin, Shahana Khan, and Aamir Sanaullah. HEWMA control chart using auxiliary information. *Iranian Journal of Science and Technology, Transactions A: Science*, 43(3):891–903, 2019.
- Syed Muhammad Muslim Raza, Maqbool Hussain Sial, Muhammad Haider, and Muhammad Moeen Butt. Hybrid exponentially weighted moving average (hewma) control chart based on exponential type estimator of mean. *Journal of Reliability and Statistical Studies*, 12(2):187–198, 2019. doi:[10.13052/jrss2229-5666.12214](https://doi.org/10.13052/jrss2229-5666.12214).
- Sadia Tariq, Muhammad Noor-ul Amin, Muhammad Hanif, and Chi-Hyuck Jun. Improved hybrid exponentially weighted moving average control chart using auxiliary information. *Journal of Reliability and Statistical Studies*, 13(1):113–125, 2020. doi:[10.13052/jrss0974-8024.1316](https://doi.org/10.13052/jrss0974-8024.1316).
- Abdul Haq, Sana Ejaz, Ming Ha Lee, and Manzoor Khan. A new double EWMA- t chart with auxiliary information for the process mean. *Quality and Reliability Engineering International*, 2021. doi:[10.1002/qre.2923](https://doi.org/10.1002/qre.2923).
- Nesma A. Saleh, Mahmoud A. Mahmoud, William H. Woodall, and Sven Knoth. A review and critique of auxiliary information-based process monitoring methods. *arXiv*, <https://arxiv.org/abs/2110.00198>, 2021.
- Michael BC Khoo, SY Teh, and Zhang Wu. Monitoring process mean and variability with one double EWMA chart. *Communications in Statistics—Theory and Methods*, 39(20):3678–3694, 2010.
- Amjad Javaid, Muhammad Noor-ul Amin, and Muhammad Hanif. A new Max-HEWMA control chart using auxiliary information. *Communications in Statistics-Simulation and Computation*, 49(5):1285–1305, 2020.
- Amjad Javaid, Muhammad Noor-ul Amin, and Muhammad Hanif. Maximum hybrid exponentially weighted moving average control chart in the presence of measurement error by using auxiliary information. *Quality and Reliability Engineering International*, 2021. doi:[10.1002/qre.2907](https://doi.org/10.1002/qre.2907).
- Sin Yin Teh, Michael BC Khoo, and Zhang Wu. A sum of squares double exponentially weighted moving average chart. *Computers & Industrial Engineering*, 61(4):1173–1188, 2011.
- Rizwan Ali and Abdul Haq. New memory-type dispersion control charts. *Quality and Reliability Engineering International*, 33(8):2131–2149, 2017.
- Saadia Tariq, Muhammad Noor ul Amin, Muhammad Aslam, and Muhammad Hanif. Design of hybrid EWMA- S^2 control chart. *Journal of Industrial and Production Engineering*, 36(8):554–562, 2019. doi:[10.1080/21681015.2019.1702111](https://doi.org/10.1080/21681015.2019.1702111).
- Muhammad Aslam, G Srinivasa Rao, Ali Hussein Al-Marshadi, and Chi-Hyuck Jun. A nonparametric hewma-p control chart for variance in monitoring processes. *Symmetry*, 11(3):356, 2019a.
- Muhammad Azam, Muhammad Aslam, and Chi-Hyuck Jun. Designing of a hybrid exponentially weighted moving average control chart using repetitive sampling. *The International Journal of Advanced Manufacturing Technology*, 77(9-12):1927–1933, 2015.
- Olatunde Adebayo Adeoti. A new double exponentially weighted moving average control chart using repetitive sampling. *International Journal of Quality & Reliability Management*, 35(2):387–404, 2018. doi:[10.1108/ijqrm-11-2016-0198](https://doi.org/10.1108/ijqrm-11-2016-0198).

- Ahmad Shafiq and Illias Musliyar. A note on “designing of a hybrid exponentially weighted moving average”. *The International Journal of Advanced Manufacturing Technology*, 97(1-4):375–377, 2018.
- Muhammad Noor-ul Amin, Navara Shabbir, Nasrullah Khan, and Afshan Riaz. Hybrid exponentially weighted moving average control chart for mean using different ranked set sampling schemes. *Kuwait Journal of Science*, 47(4):19–28, 2020.
- GA McIntyre. A method for unbiased selective sampling, using ranked sets. *Australian journal of agricultural research*, 3(4):385–390, 1952.
- Muhammad Riaz and Saddam Akber Abbasi. Nonparametric double EWMA control chart for process monitoring. *Revista Colombiana de Estadística*, 39(2):167–184, 2016. doi:[10.15446/rce.v39n2.58914](https://doi.org/10.15446/rce.v39n2.58914).
- Muhammad Ali Raza, Tahir Nawaz, Muhammad Aslam, Sajjad Haider Bhatti, and Rehan Ahmed Khan Sherwani. A new nonparametric double exponentially weighted moving average control chart. *Quality and Reliability Engineering International*, 36(1):68–87, 2020a. doi:[10.1002/qre.2560](https://doi.org/10.1002/qre.2560).
- Ambreen Shafqat, Zhensheng Huang, Muhammad Aslam, and Muhammad Shujaat Nawaz. A nonparametric repetitive sampling DEWMA control chart based on linear prediction. *IEEE Access*, 8(1):74977–74990, 2020. doi:[10.1109/access.2020.2989132](https://doi.org/10.1109/access.2020.2989132).
- Kok Ming Chan, Amitava Mukherjee, Zhi Lin Chong, and How Chinh Lee. Distribution-free double exponentially and homogeneously weighted moving average Lepage schemes with an application in monitoring exit rate. *Computers & Industrial Engineering*, 161:107370, 2021. doi:[10.1016/j.cie.2021.107370](https://doi.org/10.1016/j.cie.2021.107370).
- Lingyun Zhang, K. Govindaraju, C. D. Lai, and M. S. Bebbington. Poisson DEWMA control chart. *Communications in Statistics – Simulation and Computation*, 32(4):1265–1283, 2003a. doi:[10.1081/SAC-120023889](https://doi.org/10.1081/SAC-120023889).
- Muhammad Aslam, Nasrullah Khan, Mansour Sattam Aldosari, and Chi-Hyuck Jun. Mixed control charts using EWMA statistics. *IEEE Access*, 4:8286–8293, 2016a. doi:[10.1109/access.2016.2628915](https://doi.org/10.1109/access.2016.2628915).
- Muhammad Aslam, Nasrullah Khan, and Chi-Hyuck Jun. A hybrid exponentially weighted moving average chart for COM-Poisson distribution. *Transactions of the Institute of Measurement and Control*, 40(2):456–461, 2018a. doi:[10.1177/0142331216659920](https://doi.org/10.1177/0142331216659920).
- Vasileios Alevizakos and Christos Koukouvinos. A double exponentially weighted moving average control chart for monitoring COM-poisson attributes. *Quality and Reliability Engineering International*, 35(7):2130–2151, 2019. doi:[10.1002/qre.2494](https://doi.org/10.1002/qre.2494).
- Vasileios Alevizakos and Christos Koukouvinos. Monitoring of zero-inflated Poisson processes with EWMA and DEWMA control charts. *Quality and Reliability Engineering International*, 36(1):88–111, 2020a. doi:[10.1002/qre.2561](https://doi.org/10.1002/qre.2561).
- Vasileios Alevizakos and Christos Koukouvinos. Monitoring of zero-inflated binomial processes with a DEWMA control chart. *Journal of Applied Statistics*, 48(7):1319–1338, 2021a. doi:[10.1080/02664763.2020.1761950](https://doi.org/10.1080/02664763.2020.1761950).
- Vasileios Alevizakos and Christos Koukouvinos. A double exponentially weighted moving average chart for time between events. *Communications in Statistics – Simulation and Computation*, 49(10):2765–2784, 2020b. doi:[10.1080/03610918.2018.1532516](https://doi.org/10.1080/03610918.2018.1532516).
- Syed Muhammad Muslim Raza, Sajid Ali, Ismail Shah, Lichen Wang, and Zhen Yue. On efficient monitoring of Weibull lifetimes using censored median hybrid DEWMA chart. *Complexity*, 2020(9232506):1–10, 2020b. doi:[10.1155/2020/9232506](https://doi.org/10.1155/2020/9232506).
- Olatunde A Adeoti. On control chart for monitoring exponentially distributed quality characteristic. *Transactions of the Institute of Measurement and Control*, 42(2):295–305, 2020. doi:[10.1177/0142331219868595](https://doi.org/10.1177/0142331219868595).
- Berihun Bizuneh and Fu-Kwun Wang. A double exponentially weighted moving average chart based on likelihood ratio for monitoring an inflated Pareto process. *Quality and Reliability Engineering International*, 35(6):1698–1715, 2019. doi:[10.1002/qre.2469](https://doi.org/10.1002/qre.2469).
- Galal M. Abdella, Jinho Kim, Khalifa N. Al-Khalifa, and Abdel Magid Hamouda. Double EWMA-based polynomial quality profiles monitoring. *Quality and Reliability Engineering International*, 32(8):2639–2652, 2016. doi:[10.1002/qre.2093](https://doi.org/10.1002/qre.2093).
- Saad Alkahtani and Jay Schaffer. A double multivariate exponentially weighted moving average (dMEWMA) control chart for a process location monitoring. *Communications in Statistics – Simulation and Computation*, 41(2):238–252, 2012. doi:[10.1080/03610918.2011.585004](https://doi.org/10.1080/03610918.2011.585004).

- Sasigarn Kuvattana. Performance comparison of the Hotelling's T^2 and DMEWMA control charts using bivariate copulas for small shifts. *Thai Journal of Science and Technology*, 9:752–760, 2020. doi:[10.14456/TJST.2020.78](https://doi.org/10.14456/TJST.2020.78).
- Vasileios Alevizakos, Kashinath Chatterjee, and Christos Koukouvinos. Nonparametric triple exponentially weighted moving average signed-rank control chart for monitoring shifts in the process location. *Quality and Reliability Engineering International*, 37(6):2622–2645, 2021b. doi:[10.1002/qre.2879](https://doi.org/10.1002/qre.2879).
- Vasileios Alevizakos, Kashinath Chatterjee, and Christos Koukouvinos. A nonparametric triple exponentially weighted moving average sign control chart. *Quality and Reliability Engineering International*, 37(4):1504–1523, 2021c. doi:[10.1002/qre.2810](https://doi.org/10.1002/qre.2810).
- Tokelo Irene Letshedi, Jean-Claude Malela-Majika, Philippe Castagliola, and Sandile Charles Shongwe. Distribution-free triple EWMA control chart for monitoring the process location using the wilcoxon rank-sum statistic with fast initial response feature. *Quality and Reliability Engineering International*, 37(5):1996–2013, 2021. doi:[10.1002/qre.2842](https://doi.org/10.1002/qre.2842).
- Vasileios Alevizakos, Kashinath Chatterjee, and Christos Koukouvinos. A triple exponentially weighted moving average control chart for monitoring time between events. *Quality and Reliability Engineering International*, 37(3):1059–1079, 2021d. doi:[10.1002/qre.2781](https://doi.org/10.1002/qre.2781).
- Kashinath Chatterjee, Christos Koukouvinos, and Angeliki Lappa. A new S^2 -TEWMA control chart for monitoring process dispersion. *Quality and Reliability Engineering International*, 37(4):1334–1354, 2021. doi:[10.1002/qre.2798](https://doi.org/10.1002/qre.2798).
- Sajid Ali, SyedMuhammad Muslim Raza, Muhammad Aslam, and Muhammad Moeen Butt. CEV-hybrid DEWMA charts for censored data using Weibull distribution. *Communications in Statistics – Simulation and Computation*, 50(2):446–461, 2021a. doi:[10.1080/03610918.2018.1563147](https://doi.org/10.1080/03610918.2018.1563147).
- Shey-Huei Sheu and Tse-Chieh Lin. The generally weighted moving average control chart for detecting small shifts in the process mean. *Quality Engineering*, 16(2):209–231, 2003. doi:[10.1081/QEN-120024009](https://doi.org/10.1081/QEN-120024009).
- Kutele Mabude, Jean-Claude Malela-Majika, Philippe Castagliola, and Sandile C. Shongwe. Generally weighted moving average monitoring schemes: overview and perspectives. *Quality and Reliability Engineering International*, 37(2):409–432, 2021. doi:[10.1002/qre.2765](https://doi.org/10.1002/qre.2765).
- Shey-Huei Sheu and Yu-Tai Hsieh. The extended GWMA control chart. *J. Appl. Stat.*, 36(2):135–147, 2009. doi:[10.1080/02664760802443913](https://doi.org/10.1080/02664760802443913).
- Wen-Chih Chiu and Shey-Huei Sheu. Fast initial response features for Poisson GWMA control charts. *Communications in Statistics – Simulation and Computation*, 37(7):1422–1439, 2008. doi:[10.1080/03610910801990033](https://doi.org/10.1080/03610910801990033).
- Wen-Chih Chiu and Shin-Li Lu. On the steady-state performance of the Poisson double GWMA control chart. *Quality Technology & Quantitative Management*, 12(2):195–208, 2015. doi:[10.1080/16843703.2015.11673376](https://doi.org/10.1080/16843703.2015.11673376).
- Jen-Hsiang Chen. A double generally weighted moving average chart for monitoring the COM-poisson processes. *Symmetry*, 12(6):1014, 2020. doi:[10.3390/sym12061014](https://doi.org/10.3390/sym12061014).
- Chi-Jui Huang, Shih-Hung Tai, and Shin-Li Lu. Measuring the performance improvement of a double generally weighted moving average control chart. *Expert Systems with Applications*, 41(7):3313–3322, 2014. doi:[10.1016/j.eswa.2013.11.023](https://doi.org/10.1016/j.eswa.2013.11.023).
- Vasileios Alevizakos, Christos Koukouvinos, and Angeliki Lappa. Monitoring of time between events with a double generally weighted moving average control chart. *Quality and Reliability Engineering International*, 35(2):685–710, 2019. doi:[10.1002/qre.2430](https://doi.org/10.1002/qre.2430).
- Shin-Li Lu. Non parametric double generally weighted moving average sign charts based on process proportion. *Communications in Statistics – Theory and Methods*, 47(11):2684–2700, 2018. doi:[10.1080/03610926.2017.1342832](https://doi.org/10.1080/03610926.2017.1342832).
- Hossein Masoumi Karakani, Schalk William Human, and Janet van Niekerk. A double generally weighted moving average exceedance control chart. *Quality and Reliability Engineering International*, 35(1):224–245, 2019. doi:[10.1002/qre.2393](https://doi.org/10.1002/qre.2393).
- Michael Boon Chong Khoo, Philippe Castagliola, J. Y. Liew, W. L. Teoh, and Petros E. Maravelakis. A study on EWMA charts with runs rules – the Markov chain approach. *Communications in Statistics – Theory and Methods*, 45(14):4156–4180, 2016. doi:[10.1080/03610926.2014.917187](https://doi.org/10.1080/03610926.2014.917187).
- Petros E. Maravelakis, Philippe Castagliola, and Michael B. C. Khoo. Run length properties of run rules EWMA chart using integral equations. *Quality Technology & Quantitative Management*, 16(2):129–139, 2019. doi:[10.1080/16843703.2017.1372853](https://doi.org/10.1080/16843703.2017.1372853).

- Waqas Arshad, Nasir Abbas, Muhammad Riaz, and Zawar Hussain. Simultaneous use of runs rules and auxiliary information with exponentially weighted moving average control charts. *Quality and Reliability Engineering International*, 33(2):323–336, 2017. doi:[10.1002/qre.2007](https://doi.org/10.1002/qre.2007).
- Muhammad Riaz, Nasir Abbas, and R. J. M. M. Does. Improving the performance of CUSUM charts. *Quality and Reliability Engineering International*, 27(4):415–424, 2011b. doi:[10.1002/qre.1124](https://doi.org/10.1002/qre.1124).
- Saddam Akber Abbasi, Muhammad Riaz, and Arden Miller. Enhancing the performance of CUSUM scale chart. *Computers & Industrial Engineering*, 63(2):400–409, September 2012. ISSN 0360-8352. doi:[10.1016/j.cie.2012.03.013](https://doi.org/10.1016/j.cie.2012.03.013).
- Olatunde A. Adeoti and Jean-Claude Malela-Majika. Double exponentially weighted moving average control chart with supplementary runs-rules. *Quality Technology & Quantitative Management*, 17(2):149–172, 2020. doi:[10.1080/16843703.2018.1560603](https://doi.org/10.1080/16843703.2018.1560603).
- S. W. Roberts. A comparison of some control chart procedures. *Technometrics*, 8(3):411–430, 1966. doi:[10.1080/00401706.1966.10490374](https://doi.org/10.1080/00401706.1966.10490374).
- H. B. Wong, Fah Fatt Gan, and T. C. Chang. Designs of moving average control chart. *Journal of Statistical Computation and Simulation*, 74(1):47–62, 2004. doi:[10.1080/0094965031000105890](https://doi.org/10.1080/0094965031000105890).
- Vasileios Alevizakos, Kashinath Chatterjee, Christos Koukouvinos, and Angeliki Lappa. A double moving average control chart: Discussion. *Communications in Statistics – Simulation and Computation*, 2020. doi:[10.1080/03610918.2020.1788591](https://doi.org/10.1080/03610918.2020.1788591).
- Lingyun Zhang, CD Lai, K Govindaraju, and M Bebbington. A note on average run lengths of moving average control charts. *Economic Quality Control*, 19(1):23–27, 2004.
- G Barrie Wetherill and Don W Brown. *Statistical process control*. Springer, 1991.
- Yupaporn Areepong and Saowanit Sukparungsee. An analytical arl of binomial double moving average chart. *International Journal of Pure and Applied Mathematics*, 73(4):477–488, 2011.
- S Sukparungsee and Y Areepong. Exact average run length of double moving control chart. *International Journal of Applied Mathematics & Statistics*, 52(2):152–158, 2014.
- Saowanit Sukparungsee. Average run length of double moving average control chart for zero-inflated count processes. *Far East Journal of Mathematical Sciences*, 80(1):85–103, 2013.
- Y Areepong and S Sukparungsee. Explicit expression for the average run length of double moving average scheme for zero-inflated binomial process. *International Journal of Applied Mathematics & Statistics*, 53(3):33–43, 2015.
- Yupaporn Areepong. Statistical design of double moving average scheme for zero inflated binomial process. *International Journal of Applied Physics and Mathematics*, 6(4):185–193, 2016. doi:[10.17706/ijapm.2016.6.4.185-193](https://doi.org/10.17706/ijapm.2016.6.4.185-193).
- S Phantu, S Sukparungsee, and Y Areepong. Explicit expressions of average run length of moving average control chart for poisson integer valued autoregressive model. In *Proceedings of the International MultiConference of Engineers and Computer Scientists*, volume 2, 2016.
- Suganya Phantu, Saowanit Sukparungsee, and Yupaporn Areepong. Dma chart monitoring of the first integer-valued autoregressive processes of poisson counts. *Advances and Applications in Statistics*, 52(2):97–119, 2018.
- Kobkun Raweesawat and Saowanit Sukparungsee. Explicit formulas of arl on double moving average control chart for monitoring process mean of zipinar(1) model with an excessive number of zeros. *Applied Science and Engineering Progress*, 15(3):1–12, 2021. doi:[10.14416/j.asep.2021.03.002](https://doi.org/10.14416/j.asep.2021.03.002).
- Y Areepong and C Chanant. Double moving average control chart for zero-truncated Poisson distribution. *Journal of Physics: Conference Series*, 2014(1):012001, 2021.
- Olatunde A Adeoti, Abayomi A Akomolafe, and Femi B Adebola. Monitoring process variability using double moving average control chart. *Industrial Engineering & Management Systems*, 18(2):210–221, 2019.
- Muhammad Wasim Amir, Mishal Rani, Zameer Abbas, Hafiz Zafar Nazir, Muhammad Riaz, and Noureen Akhtar. Increasing the efficiency of double moving average chart using auxiliary variable. *Journal of Statistical Computation and Simulation*, 91(14):2880–2898, 2021. doi:[10.1080/00949655.2021.1909588](https://doi.org/10.1080/00949655.2021.1909588).
- Vasileios Alevizakos, Kashinath Chatterjee, and Christos Koukouvinos. The triple moving average control chart. *Journal of Computational and Applied Mathematics*, 384:113171, 2021e. doi:[10.1016/j.cam.2020.113171](https://doi.org/10.1016/j.cam.2020.113171).

- Vasileios Alevizakos, Kashinath Chatterjee, and Christos Koukouvinos. The quadruple moving average control chart for monitoring the process mean. *Communications in Statistics – Theory and Methods*, 2021f. doi:[10.1080/03610926.2021.1962351](https://doi.org/10.1080/03610926.2021.1962351).
- Nasir Abbas, Raja Fawad Zafar, Muhammad Riaz, and Zawar Hussain. Progressive mean control chart for monitoring process location parameter. *Quality and Reliability Engineering International*, 29(3):357–367, 2012. doi:[10.1002/qre.1386](https://doi.org/10.1002/qre.1386).
- Nasir Abbas. Progressive mean as a special case of exponentially weighted moving average. *Quality and Reliability Engineering International*, 31(4):719–720, 2015. doi:[10.1002/qre.1613](https://doi.org/10.1002/qre.1613).
- Giovanna Capizzi and Guido Masarotto. An adaptive exponentially weighted moving average control chart. *Technometrics*, 45(3):199–207, 2003. doi:[10.1198/004017003000000023](https://doi.org/10.1198/004017003000000023).
- Raja Fawad Zafar, Michael B. C. Khoo, Sajal Saha, and Zhi Lin Chong. Progressive mean control chart is not a special case of an exponentially weighted moving average control chart. *Quality and Reliability Engineering International*, 37(6):2329–2333, 2021. doi:[10.1002/qre.2886](https://doi.org/10.1002/qre.2886).
- Mohammad Saber Fallah Nezhad and Seyed Taghi Akhavan Niaki. A new monitoring design for univariate statistical quality control charts. *Information Sciences*, 180(6):1051–1059, 2010. doi:[10.1016/j.ins.2009.11.033](https://doi.org/10.1016/j.ins.2009.11.033).
- Muhammad Aslam, Rashad A. R. Bantan, and Nasrullah Khan. Monitoring the process based on belief statistic for neutrosophic gamma distributed product. *Processes*, 7(4):209, 1–17, 2019b. doi:[10.3390/pr7040209](https://doi.org/10.3390/pr7040209).
- Ahmed Ibrahim Shawky, Muhammad Aslam, and Khushnoor Khan. Multiple dependent state sampling-based chart using belief statistic under neutrosophic statistics. *Journal of Mathematics*, 2020:1–14, 2020. doi:[10.1155/2020/7680286](https://doi.org/10.1155/2020/7680286).
- Muhammad Aslam, Nasrullah Khan, and Chi-Hyuck Jun. A control chart using belief information for a gamma distribution. *Operations Research and Decisions*, 26(4):5–19, 2016b. doi:[10.5277/ORD160401](https://doi.org/10.5277/ORD160401).
- Muhammad Aslam, Nasrullah Khan, and Chi-Hyuck Jun. Designing of a control chart using belief statistic for exponential distribution. *Communications in Statistics – Simulation and Computation*, 46(5):3781–3793, 2017a. doi:[10.1080/03610918.2015.1105976](https://doi.org/10.1080/03610918.2015.1105976).
- Muhammad Riaz, Muhammad Abid, Zameer Abbas, and Hafiz Zafar Nazir. An enhanced approach for the progressive mean control charts: A discussion and comparative analysis. *Quality and Reliability Engineering International*, 37(1):1–9, 2021a. doi:[10.1002/qre.2733](https://doi.org/10.1002/qre.2733).
- Vasileios Alevizakos and Christos Koukouvinos. A double progressive mean control chart for monitoring Poisson observations. *Journal of Computational and Applied Mathematics*, 373(112232), 2020c. doi:[10.1016/j.cam.2019.04.012](https://doi.org/10.1016/j.cam.2019.04.012).
- Zameer Abbas, Hafiz Zafar Nazir, and Muhammad Riaz. On correct expression of variance of double progressive mean statistic for monitoring Poisson observations. *Quality and Reliability Engineering International*, mar 2021a. doi:[10.1002/qre.2871](https://doi.org/10.1002/qre.2871).
- Zameer Abbas, Hafiz Zafar Nazir, Muhammad Riaz, Muhammad Abid, and Noureen Akhtar. An efficient nonparametric double progressive mean chart for monitoring of the process location. *Communications in Statistics – Simulation and Computation*, apr 2021b. doi:[10.1080/03610918.2021.1910299](https://doi.org/10.1080/03610918.2021.1910299).
- Vasileios Alevizakos and Christos Koukouvinos. Monitoring reliability for a gamma distribution with a double progressive mean control chart. *Quality and Reliability Engineering International*, 37(1):199–218, 2021b. doi:[10.1002/qre.2730](https://doi.org/10.1002/qre.2730).
- Jimoh Olawale Ajadi, Kevin Hung, Muhammad Riaz, Nurudeen Ayobami Ajadi, and Tahir Mahmood. On the multivariate progressive control chart for effective monitoring of covariance matrix. *Quality and Reliability Engineering International*, 37(6):2724–2737, 2021. doi:[10.1002/qre.2887](https://doi.org/10.1002/qre.2887).
- Nasir Abbas. Homogeneously weighted moving average control chart with an application in substrate manufacturing process. *Computers & Industrial Engineering*, 120:460–470, 2018. doi:[10.1016/j.cie.2018.05.009](https://doi.org/10.1016/j.cie.2018.05.009).
- Muhammad Abid, Aroosa Shabbir, Hafiz Zafar Nazir, Rehan Ahmed Khan Sherwani, and Muhammad Riaz. A double homogeneously weighted moving average control chart for monitoring of the process mean. *Quality and Reliability Engineering International*, 36(5):1513–1527, 2020. doi:[10.1002/qre.2641](https://doi.org/10.1002/qre.2641).
- Olatunde Adebayo Adeoti and Sunday Olawale Koleoso. A hybrid homogeneously weighted moving average control chart for process monitoring. *Quality and Reliability Engineering International*, 36(6):2170–2186, jun 2020. doi:[10.1002/qre.2690](https://doi.org/10.1002/qre.2690).

- Vasileios Alevizakos, Kashinath Chatterjee, and Christos Koukouvinos. The extended homogeneously weighted moving average control chart. *Quality and Reliability Engineering International*, 37(5):2134–2155, 2021g. doi:[10.1002/qre.2849](https://doi.org/10.1002/qre.2849).
- Jean-Claude Malela-Majika, Sandile Charles Shongwe, and Olatunde Adebayo Adeoti. A hybrid homogeneously weighted moving average control chart for process monitoring: discussion. *Quality and Reliability Engineering International*, may 2021. doi:[10.1002/qre.2911](https://doi.org/10.1002/qre.2911).
- Syed Masroor Anwar, Muhammad Aslam, Babar Zaman, and Muhammad Riaz. An enhanced double homogeneously weighted moving average control chart to monitor process location with application in automobile field. *Quality and Reliability Engineering International*, 2021a. doi:[10.1002/qre.2966](https://doi.org/10.1002/qre.2966).
- Muhammad Riaz, Muhammad Abid, Aroosa Shabbir, Hafiz Zafar Nazir, Zameer Abbas, and Saddam Akber Abbasi. A non-parametric double homogeneously weighted moving average control chart under sign statistic. *Quality and Reliability Engineering International*, 37(4):1544–1560, 2021b. doi:[10.1002/qre.2812](https://doi.org/10.1002/qre.2812).
- Vasileios Alevizakos, Kashinath Chatterjee, and Christos Koukouvinos. An extended nonparametric homogeneously weighted moving average sign control chart. *Quality and Reliability Engineering International*, may 2021h. doi:[10.1002/qre.2924](https://doi.org/10.1002/qre.2924).
- Muhammad Riaz, Zameer Abbas, Hafiz Zafar Nazir, and Muhammad Abid. On the development of triple homogeneously weighted moving average control chart. *Symmetry*, 13(2):360, 2021c. doi:[10.3390/sym13020360](https://doi.org/10.3390/sym13020360).
- Babar Zaman, Muhammad Riaz, Nasir Abbas, and Ronald JMM Does. Mixed cumulative sum–exponentially weighted moving average control charts: an efficient way of monitoring process location. *Quality and Reliability Engineering International*, 31(8):1407–1421, 2015.
- Babar Zaman, Nasir Abbas, Muhammed Riaz, and Muhammad Hisyam Lee. Mixed CUSUM-EWMA chart for monitoring process dispersion. *The International Journal of Advanced Manufacturing Technology*, 86(9):3025–3039, 2016.
- Babar Zaman, Muhammad Riaz, and Muhammad Hisyam Lee. On the performance of control charts for simultaneous monitoring of location and dispersion parameters. *Quality and Reliability Engineering International*, 33(1):37–56, 2017.
- Jimoh Olawale Ajadi, Muhammad Riaz, and Khalid Al-Ghamdi. On increasing the sensitivity of mixed EWMA–CUSUM control charts for location parameter. *Journal of Applied Statistics*, 43(7):1262–1278, 2016.
- Hafiz Zafar Nazir, Nasir Abbas, Muhammad Riaz, and Ronald JMM Does. A comparative study of memory-type control charts under normal and contaminated normal environments. *Quality and Reliability Engineering International*, 32(4):1347–1356, 2016.
- Muhammad Abid, Hafiz Zafar Nazir, Muhammad Riaz, and Zhengyan Lin. In-control robustness comparison of different control charts. *Transactions of the Institute of Measurement and Control*, 40(13):3860–3871, 2018.
- Shahid Hussain, Xiaoguang Wang, Shabbir Ahmad, and Muhammad Riaz. On a class of mixed EWMA–CUSUM median control charts for process monitoring. *Quality and Reliability Engineering International*, 36(3):910–946, 2020.
- Syed Masroor Anwar, Muhammad Aslam, Muhammad Riaz, and Babar Zaman. On mixed memory control charts based on auxiliary information for efficient process monitoring. *Quality and Reliability Engineering International*, 36(6):1949–1968, 2020. doi:[10.1002/qre.2667](https://doi.org/10.1002/qre.2667).
- Syed Masroor Anwar, Muhammad Aslam, Babar Zaman, and Muhammad Riaz. Mixed memory control chart based on auxiliary information for simultaneously monitoring of process parameters: An application in glass field. *Computers & Industrial Engineering*, 156:107284, 2021b. doi:[10.1016/j.cie.2021.107284](https://doi.org/10.1016/j.cie.2021.107284).
- Atieh Mohamadkhani and Amir Hossein Amiri. Developing mixed EWMA-CUSUM and CUSUM-EWMA control charts based on MRSS and DRSS procedures. *Scientia Iranica*, 2020. doi:[10.24200/sci.2020.55632.4328](https://doi.org/10.24200/sci.2020.55632.4328).
- Muhammad Aslam. A mixed EWMA–CUSUM control chart for Weibull-distributed quality characteristics. *Quality and Reliability Engineering International*, 32(8):2987–2994, 2016.
- Jean-Claude Malela-Majika and Eeva Rapoo. Distribution-free mixed cumulative sum-exponentially weighted moving average control charts for detecting mean shifts. *Quality and Reliability Engineering International*, 33(8):1983–2002, 2017. doi:[10.1002/qre.2162](https://doi.org/10.1002/qre.2162).
- Richard Osei-Aning, Saddam Akber Abbasi, and Muhammad Riaz. Mixed EWMA-CUSUM and mixed CUSUM-EWMA modified control charts for monitoring first order autoregressive processes. *Quality Technology & Quantitative Management*, 14(4):429–453, 2017.

- Nasir Abbas, Ishaq A Raji, Muhammad Riaz, and Khalid Al-Ghamdi. On designing mixed EWMA dual-CUSUM chart with applications in petro-chemical industry. *IEEE Access*, 6:78931–78946, 2018. doi:[10.1109/access.2018.2885598](https://doi.org/10.1109/access.2018.2885598).
- Muhammad Riaz, Qurat-Ul-Ain Khaliq, and Shahla Gul. Mixed Tukey EWMA-CUSUM control chart and its applications. *Quality Technology & Quantitative Management*, 14(4):378–411, 2017.
- Abdul Haq. A novel cumulative EWMA-sum mean chart. *Quality and Reliability Engineering International*, 2021. doi:[10.1002/qre.2991](https://doi.org/10.1002/qre.2991).
- Jimoh Olawale Ajadi and Muhammad Riaz. Mixed multivariate EWMA-CUSUM control charts for an improved process monitoring. *Communications in Statistics – Theory and Methods*, 46(14):6980–6993, 2017.
- Muhammad Riaz, Jimoh Olawale Ajadi, Tahir Mahmood, and Saddam Akber Abbasi. Multivariate mixed EWMA-CUSUM control chart for monitoring the process variance-covariance matrix. *IEEE Access*, 7:100174–100186, 2019.
- Babar Zaman, Muhammad Hisyam Lee, Muhammad Riaz, and Mu’azu Ramat Abujiya. An improved process monitoring by mixed multivariate memory control charts: An application in wind turbine field. *Computers & Industrial Engineering*, 142:106343, 2020. doi:[10.1016/j.cie.2020.106343](https://doi.org/10.1016/j.cie.2020.106343).
- Nasrullah Khan, Muhammad Aslam, and Chi-Hyuck Jun. A EWMA control chart for exponential distributed quality based on moving average statistics. *Quality and Reliability Engineering International*, 32(3):1179–1190, 2016.
- Liaquat Ahmad, Muhammad Aslam, Nasrullah Khan, and Chi-Hyuck Jun. Double moving average control chart for exponential distributed life using EWMA. In *AIP Conference Proceedings*, volume 1905, page 050003. AIP Publishing LLC, 2017. doi:[10.1063/1.5012222](https://doi.org/10.1063/1.5012222).
- Rattikarn Taboran, Saowanit Sukparungsee, and Yupaporn Areepong. Mixed moving average-exponentially weighted moving average control charts for monitoring of parameter change. In *Proceedings of the International MultiConference of Engineers and Computer Scientists (IMECS) 2019*, 2019.
- Saowanit Sukparungsee, Yupaporn Areepong, and Rattikarn Taboran. Exponentially weighted moving average—moving average charts for monitoring the process mean. *Plos one*, 15(2):e0228208, 2020. doi:[10.1371/journal.pone.0228208](https://doi.org/10.1371/journal.pone.0228208).
- Muhammad Aslam. An insight into control charts using EWMA. *Communications in Statistics – Theory and Methods*, 2021. doi:[10.1080/03610926.2021.1928705](https://doi.org/10.1080/03610926.2021.1928705).
- Muhammad Aslam, Wenhao Gui, Nasrullah Khan, and Chi-Hyuck Jun. Double moving average–EWMA control chart for exponentially distributed quality. *Communications in Statistics – Simulation and Computation*, 46(9):7351–7364, 2017b.
- Shin-Li Lu. Novel design of composite generally weighted moving average and cumulative sum charts. *Quality and Reliability Engineering International*, 33(8):2397–2408, 2017. doi:[10.1002/qre.2197](https://doi.org/10.1002/qre.2197).
- Rizwan Ali and Abdul Haq. A mixed GWMA–CUSUM control chart for monitoring the process mean. *Communications in Statistics – Theory and Methods*, 47(15):3779–3801, 2018a.
- Rizwan Ali and Abdul Haq. New GWMA-CUSUM control chart for monitoring the process dispersion. *Quality and Reliability Engineering International*, 34(6):997–1028, 2018b.
- Chi-Jui Huang, Shin-Li Lu, and Jen-Hsiang Chen. Enhanced generally weighted moving average variance charts for monitoring process variance with individual observations. *Quality and Reliability Engineering International*, 36(1):285–302, 2020. doi:[10.1002/qre.2571](https://doi.org/10.1002/qre.2571).
- K Mabude, J-C Malela-Majika, P Castagliola, and SC Shongwe. Distribution-free mixed GWMA-CUSUM and CUSUM-GWMA Mann–Whitney charts to monitor unknown shifts in the process location. *Communications in Statistics – Simulation and Computation*, 2020. doi:[10.1080/03610918.2020.1811331](https://doi.org/10.1080/03610918.2020.1811331).
- Muhammad Aslam, Muhammad Azam, and Chi-Hyuck Jun. A HEWMA-CUSUM control chart for the Weibull distribution. *Communications in Statistics – Theory and Methods*, 47(24):5973–5985, 2018b.
- Hafiz Zafar Nazir, Muhammad Abid, Noreen Akhtar, Muhammad Riaz, and Sadia Qamar. An efficient mixed-memory-type control chart for normal and non-normal processes. *Scientia Iranica*, 28(3):1736–1749, 2021.
- Rattikarn Taboran, Saowanit Sukparungsee, and Yupaporn Areepong. Design of a new Tukey MA-DEWMA control chart to monitor process and its applications. *IEEE Access*, 9:102746–102757, 2021.

- Muhammad Abid, Sun Mei, Hafiz Zafar Nazir, Muhammad Riaz, and Shahid Hussain. A mixed HWMA-CUSUM mean chart with an application to manufacturing process. *Quality and Reliability Engineering International*, 37(2):618–631, 2021a. doi:[10.1002/qre.2752](https://doi.org/10.1002/qre.2752).
- Muhammad Abid, Sun Mei, Hafiz Zafar Nazir, Muhammad Riaz, Shahid Hussain, and Zameer Abbas. A mixed cumulative sum homogeneously weighted moving average control chart for monitoring process mean. *Quality and Reliability Engineering International*, 37(5):1758–1771, 2021b. doi:[10.1002/qre.2824](https://doi.org/10.1002/qre.2824).
- Zameer Abbas, Hafiz Zafar Nazir, Noureen Akhtar, Muhammad Riaz, and Muhammad Abid. On developing an exponentially weighted moving average chart under progressive setup: An efficient approach to manufacturing processes. *Quality and Reliability Engineering International*, 36(7):2569–2591, 2020. doi:[10.1002/qre.2716](https://doi.org/10.1002/qre.2716).
- Vasileios Alevizakos, Kashinath Chatterjee, and Christos Koukouvinos. On developing an exponentially weighted moving average chart under progressive setup: an efficient approach to manufacturing processes—discussion. *Quality and Reliability Engineering International*, 37(4):1628–1634, 2021i. doi:[10.1002/qre.2816](https://doi.org/10.1002/qre.2816).
- Nurudeen Ayobami Ajadi, Osebekwin Asiribo, and Ganiyu Dawodu. Progressive mean exponentially weighted moving average control chart for monitoring the process location. *International Journal of Quality & Reliability Management*, 2020. doi:[10.1108/ijqrm-05-2020-0138](https://doi.org/10.1108/ijqrm-05-2020-0138).
- Saber Ali, Zameer Abbas, Hafiz Zafar Nazir, Muhammad Riaz, Xingfa Zhang, and Yuan Li. On developing sensitive nonparametric mixed control charts with application to manufacturing industry. *Quality and Reliability Engineering International*, 37(6):2699–2723, 2021b. doi:[10.1002/qre.2885](https://doi.org/10.1002/qre.2885).
- Saber Ali, Zameer Abbas, Hafiz Zafar Nazir, Muhammad Riaz, Xingfa Zhang, and Yuan Li. On designing mixed nonparametric control chart for monitoring the manufacturing processes. *Arabian Journal for Science and Engineering*, 2021c. doi:[10.1007/s13369-021-05801-6](https://doi.org/10.1007/s13369-021-05801-6).
- Muhammad Riaz, Zameer Abbas, Hafiz Zafar Nazir, Noureen Akhtar, and Muhammad Abid. On designing a progressive EWMA structure for an efficient monitoring of silicate enactment in hard bake processes. *Arabian Journal for Science and Engineering*, 46(2):1743–1760, 2021d.
- Ewan Stafford Page. Continuous inspection schemes. *Biometrika*, 41(1-2):100–115, 1954.
- Ronald B. Crosier. A new two-sided cumulative quality control scheme. *Technometrics*, 28(3):187–194, 1986. doi:[10.2307/1269074](https://doi.org/10.2307/1269074).
- S. W. Roberts. Control chart tests based on geometric moving averages. *Technometrics*, 1(3):239–250, 1959. doi:[10.1080/00401706.1959.10489860](https://doi.org/10.1080/00401706.1959.10489860).
- John F. MacGregor and Thomas J. Harris. *Discussion of: Exponentially weighted moving average control schemes: Properties and enhancements (by Lucas & Saccucci)*. *Technometrics*, 32:23–26, 1990. doi:[10.2307/1269840](https://doi.org/10.2307/1269840).
- Sven Knoth. *spc: statistical process control – collection of some useful functions*. R Foundation for Statistical Computing, Vienna, Austria, 2021. R package version 0.6.5, <https://cran.r-project.org/web/packages/spc/index.html>.
- George V. Moustakides. Optimal stopping times for detecting changes in distributions. *Ann. Stat.*, 14(4):1379–1387, 1986. doi:[10.1214/aos/1176350164](https://doi.org/10.1214/aos/1176350164).
- Bernard Phineas Dudding and William Joseph Jennett. *Quality control charts*. British Standards Institution, London, 1942.
- Hans Weiler. The use of runs to control the mean in quality control. *J. Amer. Statist. Assoc.*, 48(264):816–825, 1953. doi:[10.1080/01621459.1953.10501203](https://doi.org/10.1080/01621459.1953.10501203).
- WECO. *Statistical quality control handbook*. Western Electrical Company (WECO), Indianapolis, IN, 1956.
- Lloyd S. Nelson. Shewhart control chart – tests for special causes. *Journal of Quality Technology*, 16(4):237–239, 1984. doi:[10.1080/00224065.1984.11978921](https://doi.org/10.1080/00224065.1984.11978921).
- Morton Klein. Two alternatives to the Shewhart \bar{X} control chart. *Journal of Quality Technology*, 32(4):427–431, 2000. doi:[10.1080/00224065.2000.11980028](https://doi.org/10.1080/00224065.2000.11980028).
- Michael Boon Chong Khoo. Design of runs rules schemes. *Quality Engineering*, 16(1):27–43, 2003. doi:[10.1081/QEN-120020769](https://doi.org/10.1081/QEN-120020769).
- M. V. Koutras, Sotiris Bersimis, and Petros E. Maravelakis. Statistical process control using Shewhart control charts with supplementary runs rules. *Methodology and Computing in Applied Probability*, 9(2):207–224, 2007. doi:[10.1007/s11009-007-9016-8](https://doi.org/10.1007/s11009-007-9016-8).

- Charles W. Champ and William H. Woodall. Exact results for Shewhart control charts with supplementary runs rules. *Technometrics*, 29(4):393–399, 1987. doi:[10.2307/1269449](https://doi.org/10.2307/1269449).
- Charles W. Champ. Steady-state run length analysis of a Shewhart quality control chart with supplementary runs rules. *Communications in Statistics – Theory and Methods*, 21(3):765–777, 1992. doi:[10.1080/03610929208830813](https://doi.org/10.1080/03610929208830813).
- Nasir Abbas. *Memory-type control charts in statistical process control*. PhD thesis, University of Amsterdam, 2012. <https://dare.uva.nl/search?metis.record.id=375907>.
- Frédéric Y. Bois and Don R. Maszle. MCSim: A Monte Carlo simulation program. *Journal of Statistical Software*, 2(9):1–60, 1997. doi:[10.18637/jss.v002.i09](https://doi.org/10.18637/jss.v002.i09).
- Lingyun Zhang, K. Govindaraju, C. D. Lai, and M. S. Bebbington. Poisson DEWMA control chart. *Communications in Statistics – Simulation and Computation*, 32(4):1265–1283, 2003b. doi:[10.1081/SAC-120023889](https://doi.org/10.1081/SAC-120023889).
- William H. Woodall and Frederick W. Faltin. Rethinking control chart design and evaluation. *Quality Engineering*, 31(4):596–605, 2019. doi:[10.1080/08982112.2019.1582779](https://doi.org/10.1080/08982112.2019.1582779).